US 20070107884A1

(19) **United States**

(12) **Patent Application Publication**

(10) **Pub. No.: US 2007/0107884 A1**

(43) **Pub. Date: May 17, 2007**

Sirkar et al.

(54) **POLYMERIC HOLLOW FIBER HEAT EXCHANGE SYSTEMS**

(76) Inventors: **Kamalesh K. Sirkar**, Bridgewater, NJ (US); **Alexander P. Korikov**, Uniondale, NY (US); **Praveen B. Kosaraju**, Harrison, NJ (US); **Dimitrios Zarkadas**, Fanwood, NJ (US)

Correspondence Address:
McCARTER & ENGLISH, LLP
Attn.: Basam E. Nabulsi
Financial Centre, Suite 304A
695 East Main Street
Stamford, CT 06901-2103 (US)

(21) Appl. No.: **11/586,150**

(22) Filed: **Oct. 25, 2006**

Related U.S. Application Data

(60) Provisional application No. 60/730,954, filed on Oct. 27, 2005.

Publication Classification

(51) **Int. Cl.**
F28F 13/18 (2006.01)

(52) **U.S. Cl.** **165/133**; 165/158

(57) **ABSTRACT**

Heat exchange systems are provided that include one or more polymeric hollow fibers. Exemplary hollow fibers are asymmetric and include a microporous wall and a dense skin formed thereon, thereby preventing liquid transmission and/or contamination through the wall of the hollow fiber while simultaneously enhancing heat transfer based on the presence of liquid molecules within the porous substructure of the hollow fiber. The hollow fibers may be employed in a variety of heat transfer-related commercial/industrial applications, including solvent-aqueous systems, organic-aqueous systems, organic-organic systems, desalination applications, solar heating applications, applications in the chemical industry, applications in the biomedical industry, and applications in the biotechnology or pharmaceutical industry, e.g., extracorporeal blood oxygenation systems. Heat transfer systems wherein steam is advantageously condensed on a first side of a polymeric, hollow fiber-based heat exchanger are also provided. The condensed steam provides energy that may be used to heat water and/or other liquids that flow on a second side of the polymeric, hollow fibers.

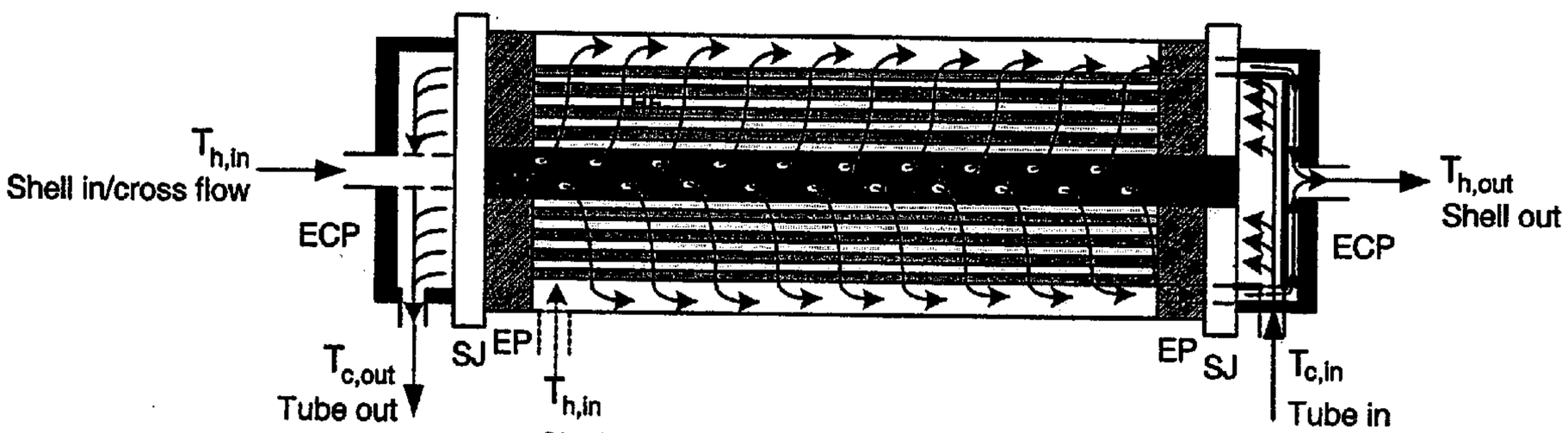

Shell in/parallel flow

CFT	Central feeder tube	HF	Hollow fibers
ECP	End cap with port	SJ	Sleeve joint
EP	Epoxy plug		

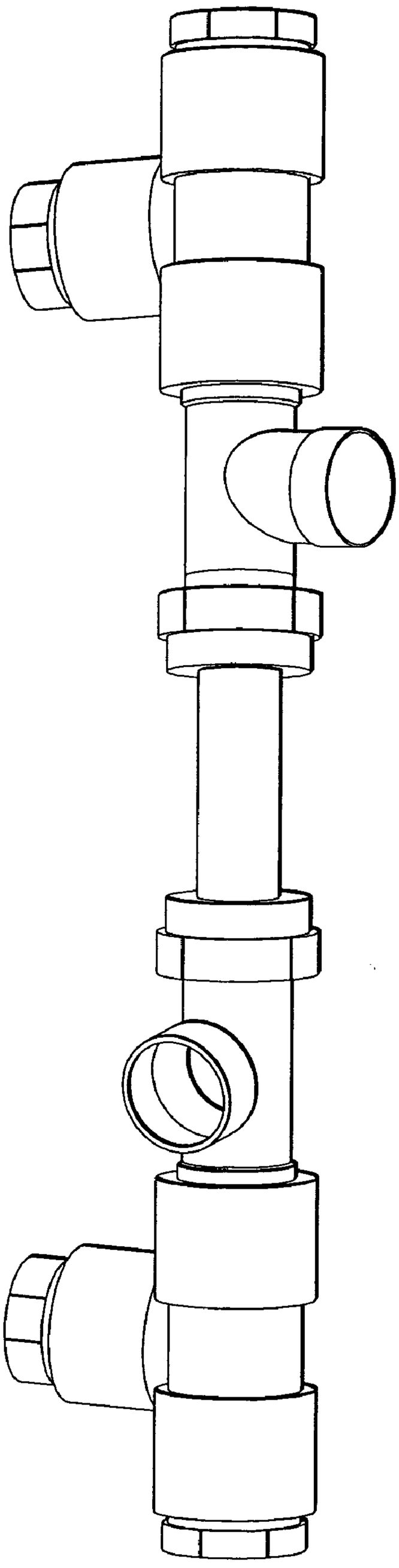

FIG. 1

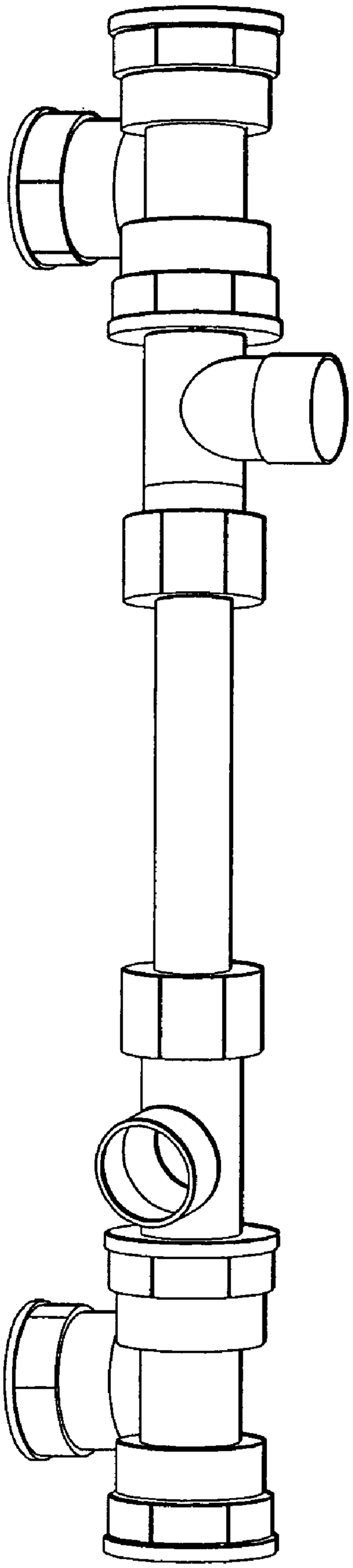

FIG. 2

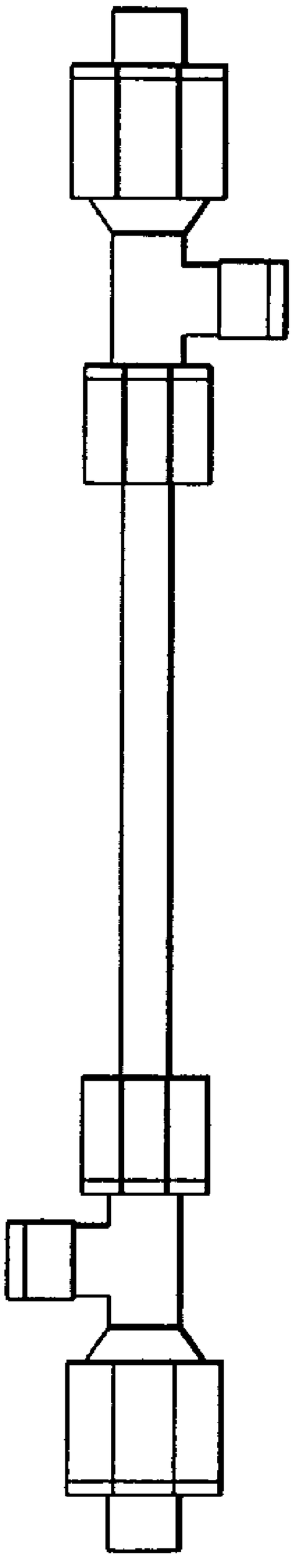

FIG. 3

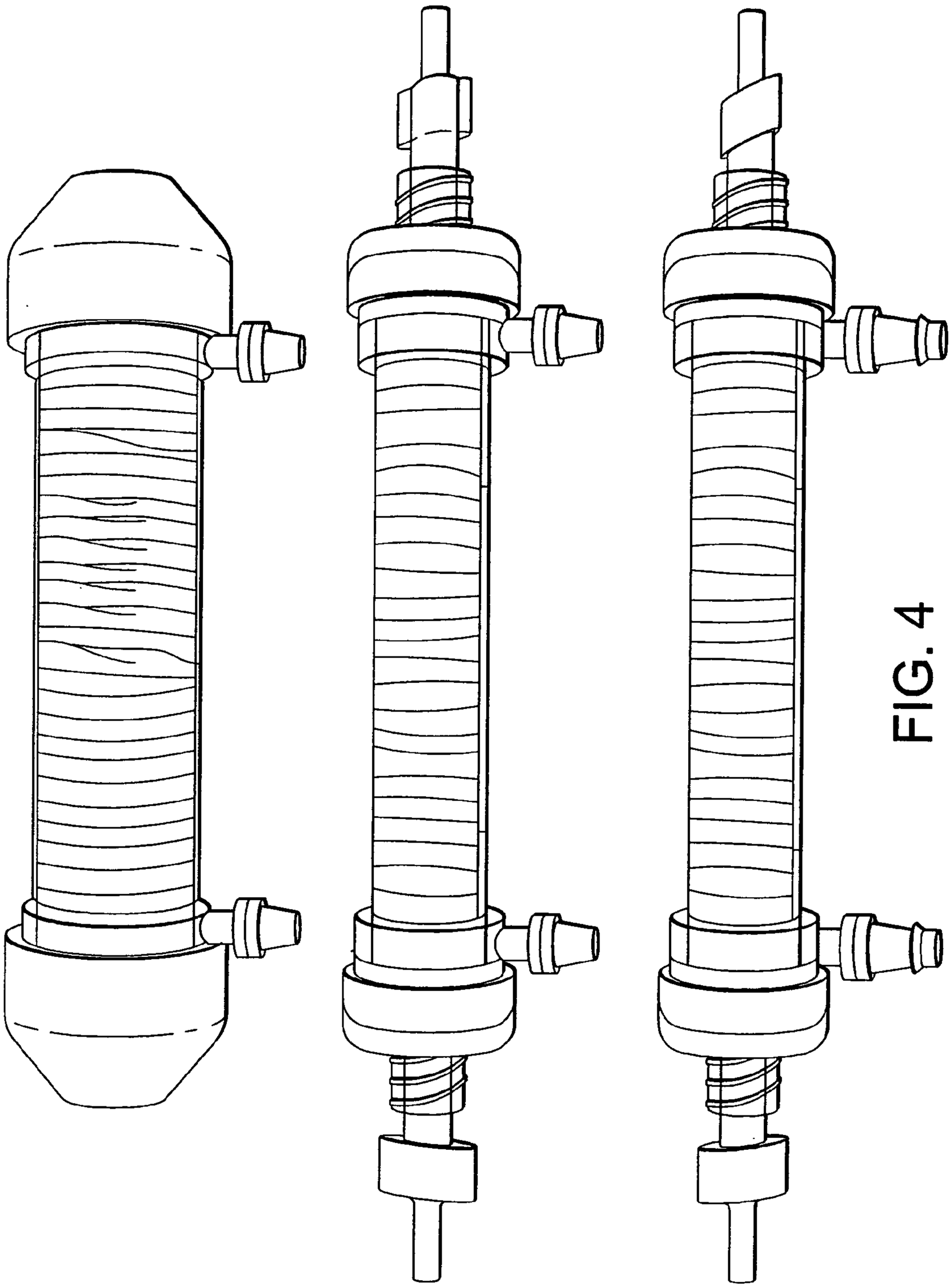

FIG. 4

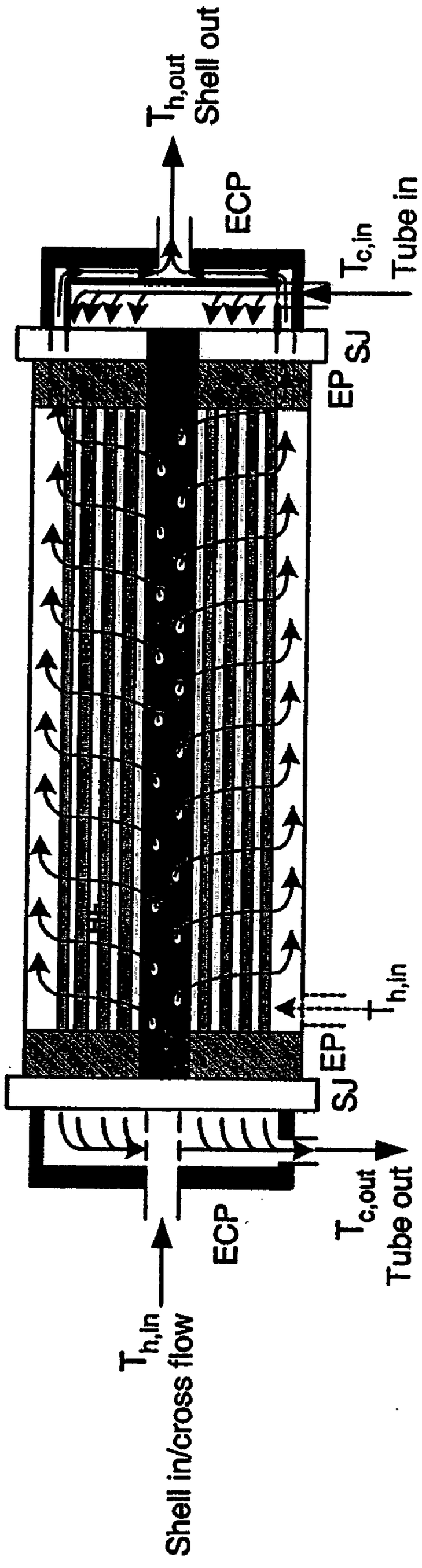
$T_{h,out}$
Shell out
ECP
$T_{c,in}$
Tube in
SJ
EP
$T_{h,in}$
Shell in/parallel flow
CFT Central feeder tube
ECP End cap with port
EP Epoxy plug
HF Hollow fibers
SJ Sleeve joint
$T_{h,in}$
Shell in/cross flow
ECP
$T_{c,out}$
Tube out

FIG. 5

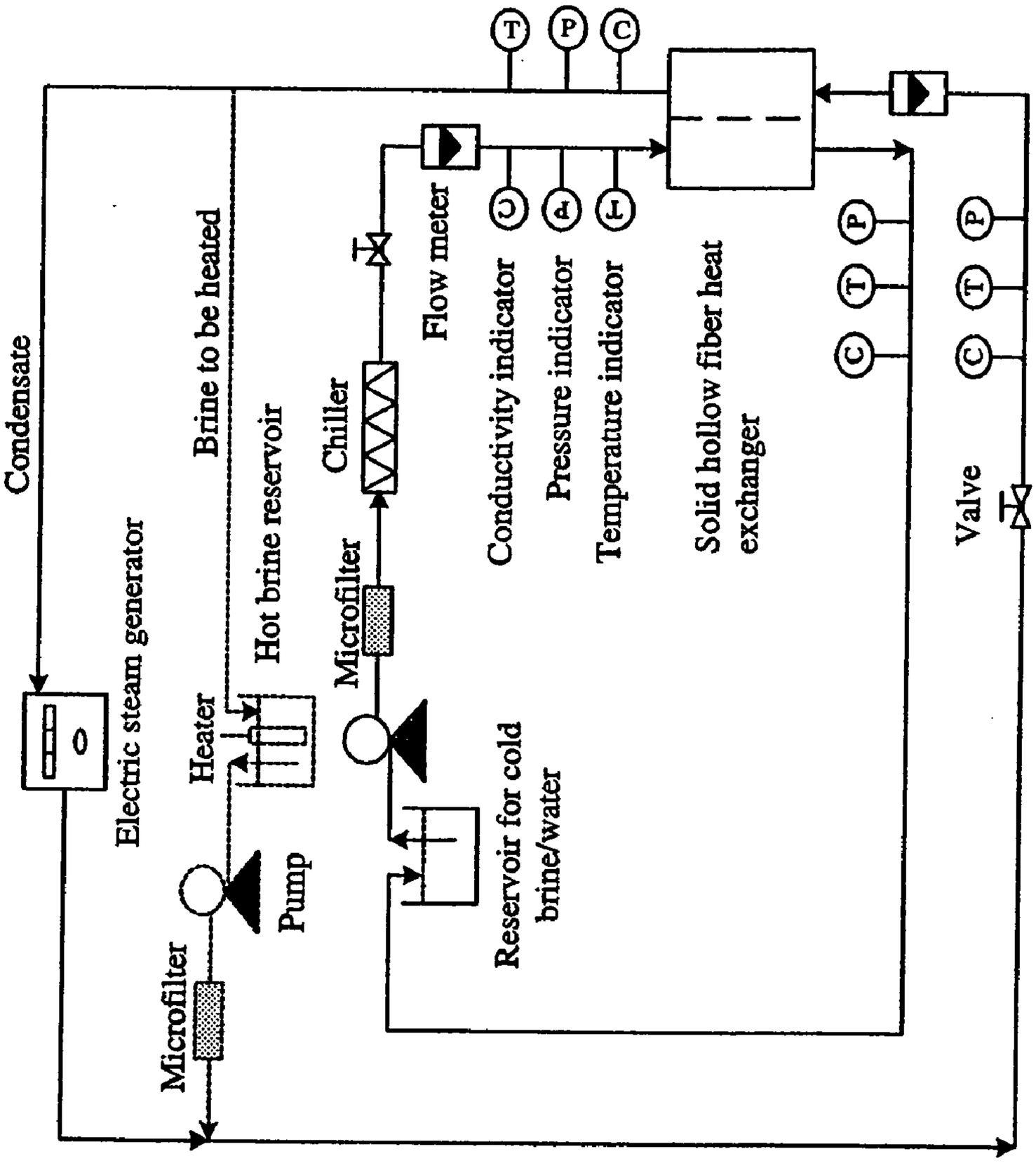
Condensate
Brine to be heated
Electric steam generator
Hot brine reservoir
Heater
Pump
Microfilter
Microfilter
Chiller
Flow meter
Conductivity indicator
Pressure indicator
Temperature indicator
Solid hollow fiber heat exchanger
Reservoir for cold brine/water
Valve
T
P
C

FIG. 6

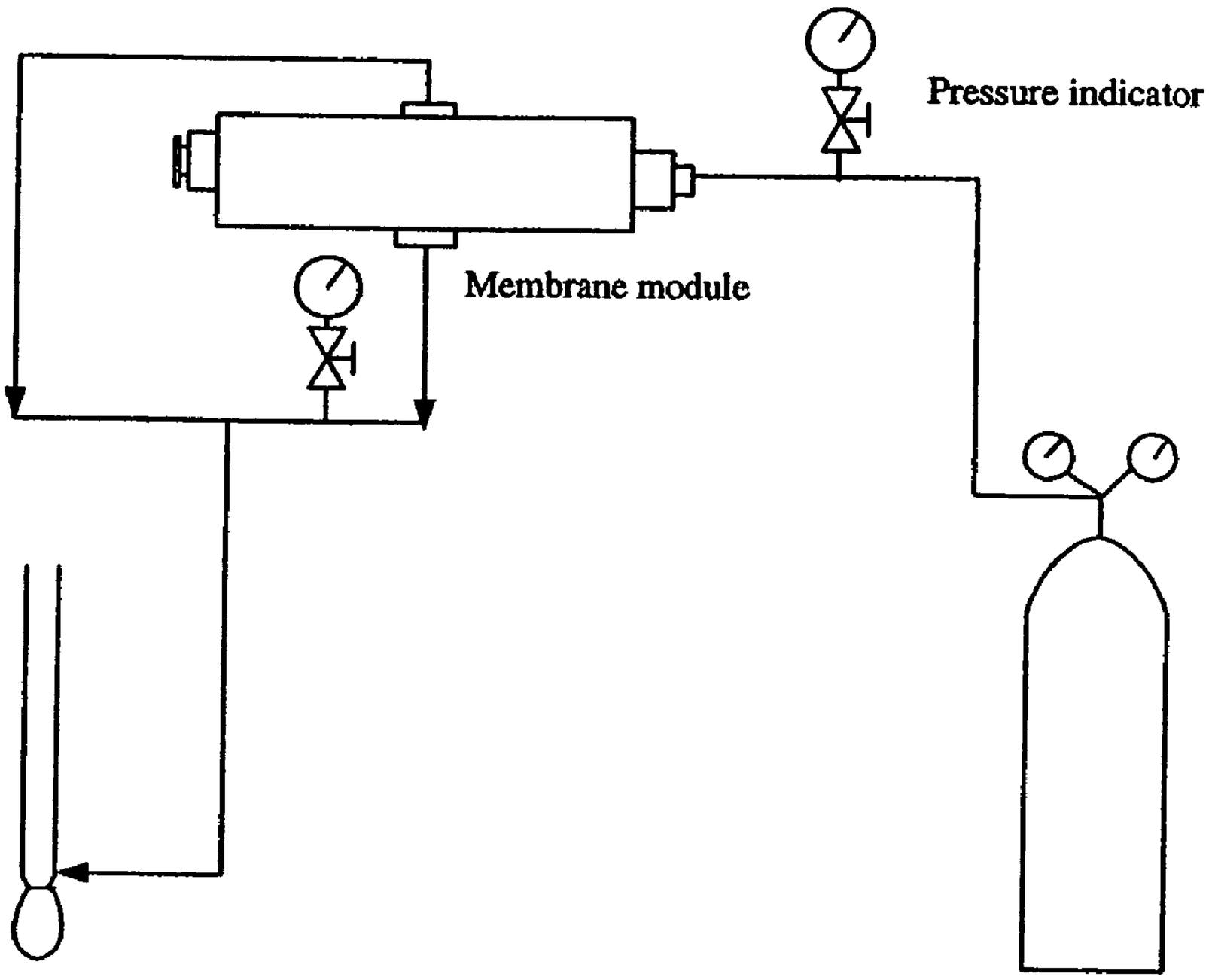
Pressure indicator
Membrane module
Bubble flow meter
Gas cylinder

FIG. 7

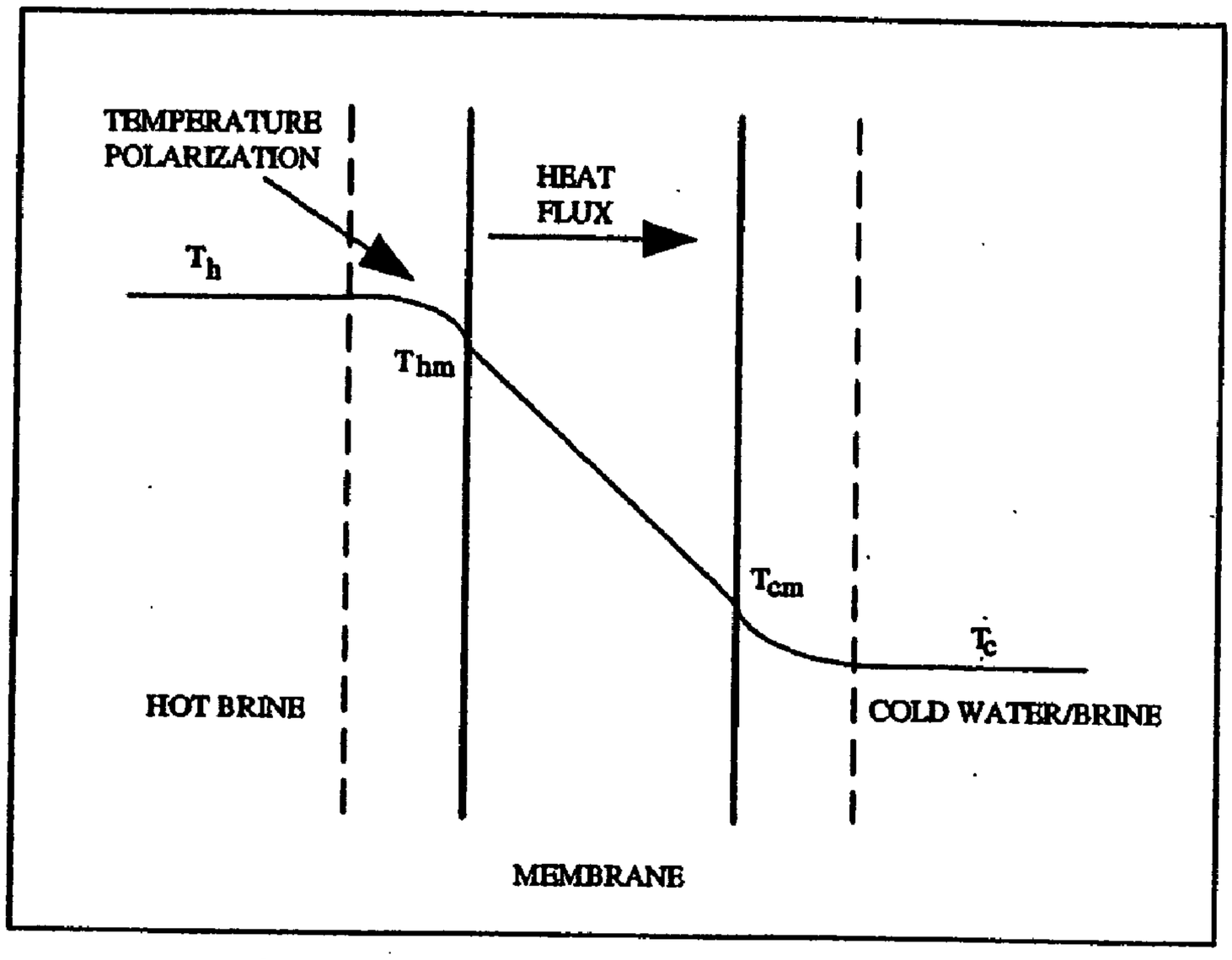
TEMPERATURE POLARIZATION
HEAT FLUX
T_h
T_{hm}
T_{cm}
T_c
HOT BRINE
COLD WATER/BRINE
MEMBRANE

FIG. 8a

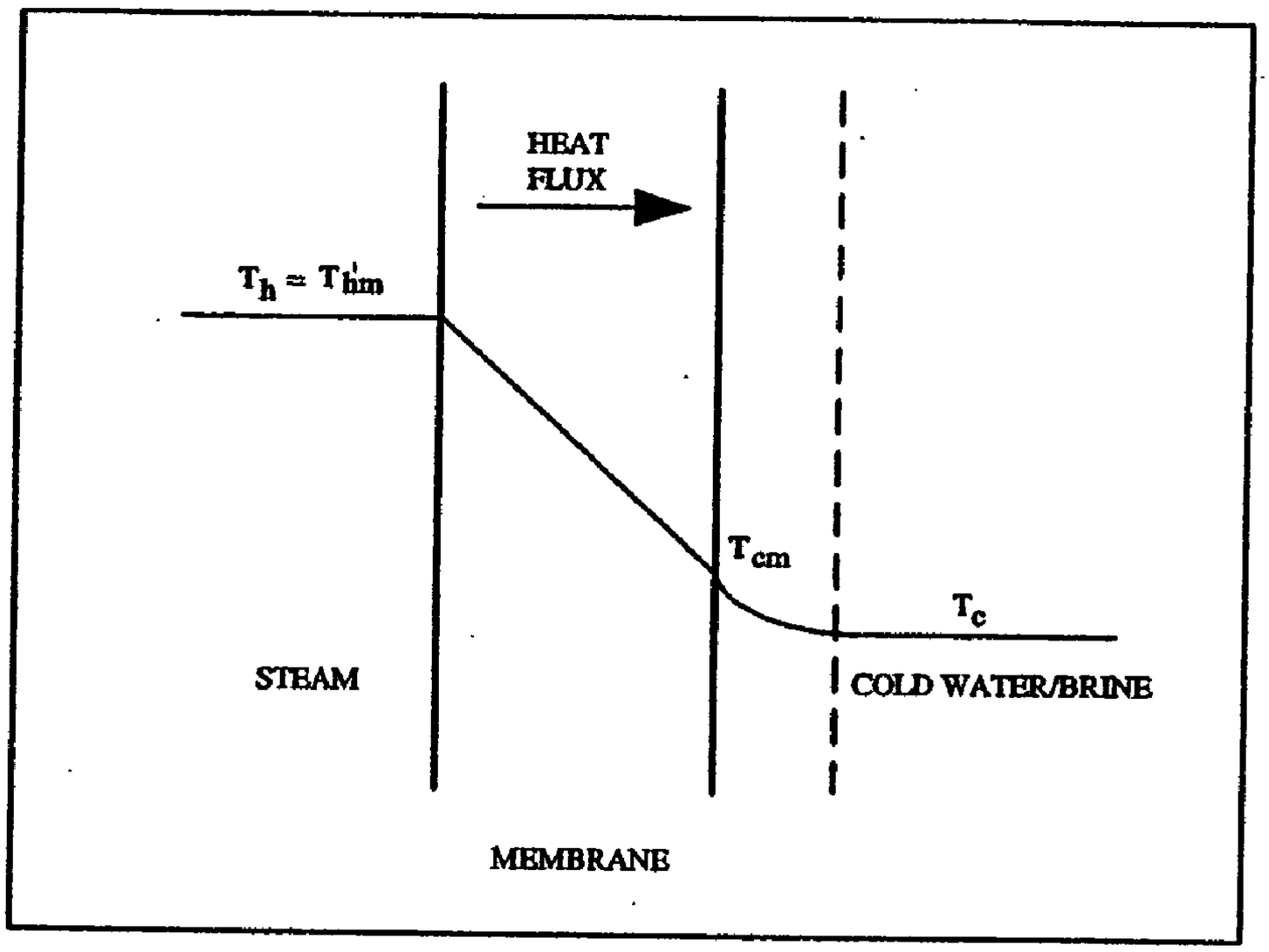
HEAT FLUX
$T_h \simeq T_{hm}'$
T_{cm}
T_c
STEAM
COLD WATER/BRINE
MEMBRANE

FIG. 8b

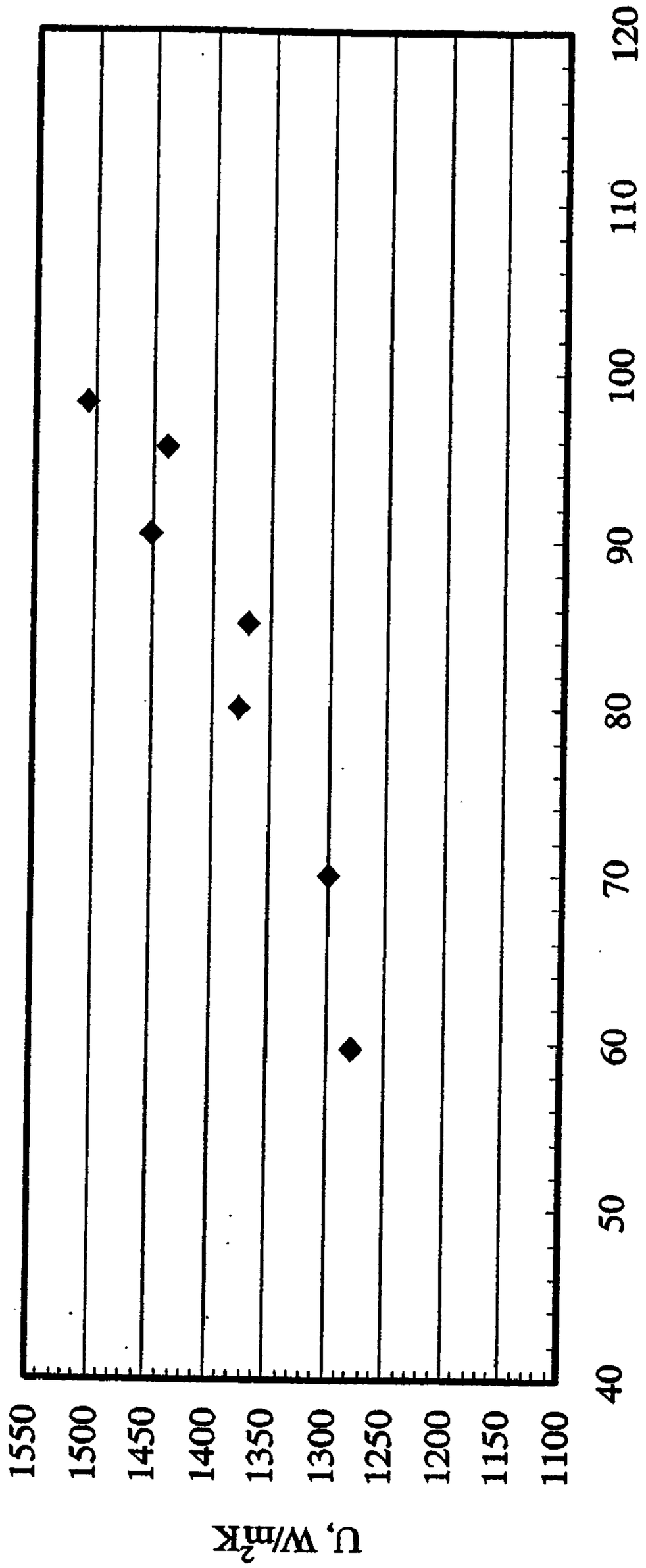

Variation of overall heat transfer coefficient of module HEPP1 (containing 79 PP fibers having I.D. 0.0425 cm, O.D.0.0575 cm and I.D. surface area 195 cm^2) with feed inlet temperature (Feed: 4% NaCl solution flowing (crossflow) on the shell side with interstitial velocity of 150 cm/min; cooling water: D.I. water flowing through the tube side with linear velocity of 4300 cm/min at inlet temperature of 27°C)

FIG. 9

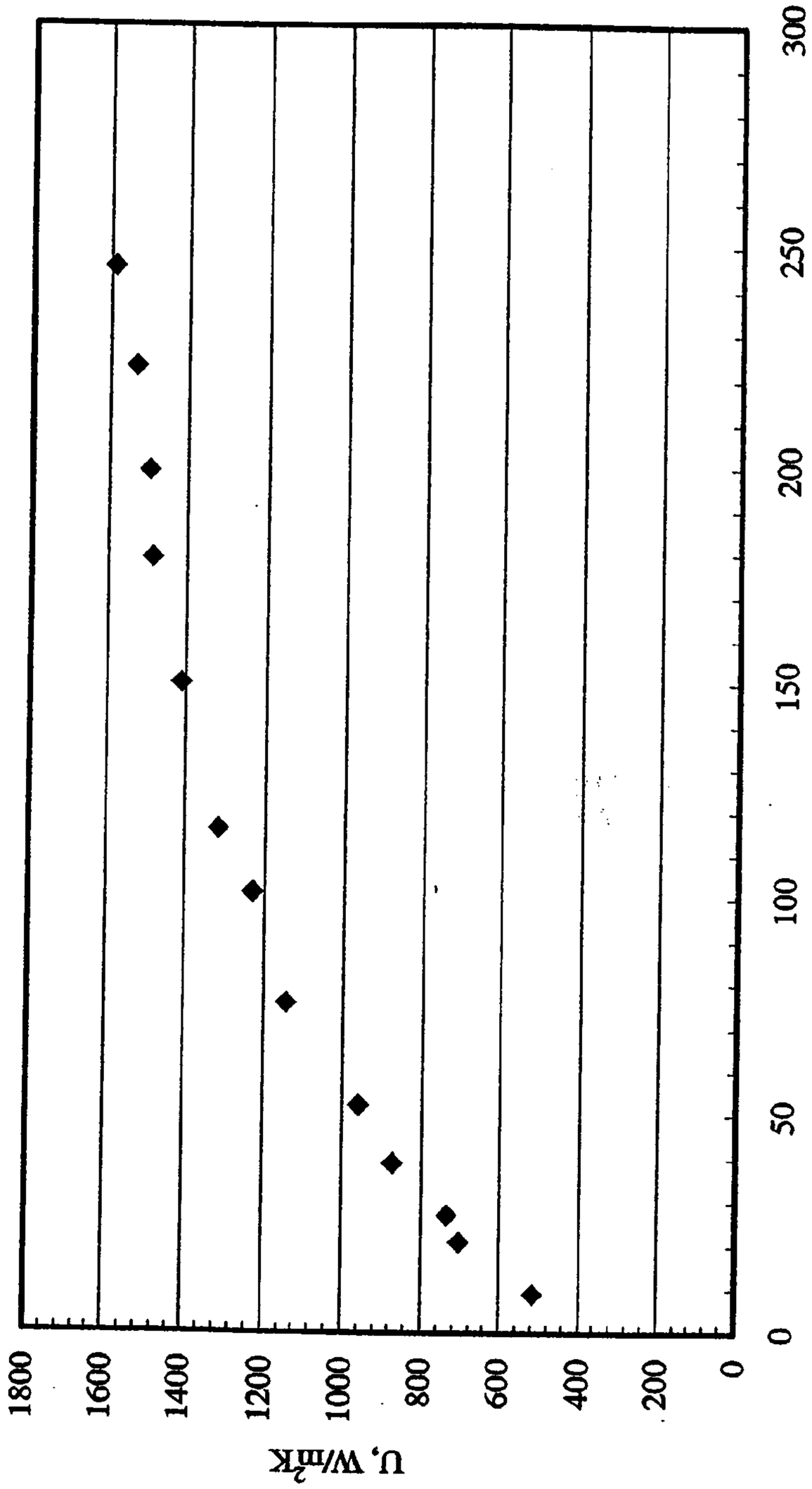

Variation of overall heat transfer coefficient of module HEPP1 (containing 79 PP fibers having I.D. 0.0425 cm, O.D.0.0575 cm and I.D. surface area 195 cm^2) with interstitial velocity of hot brine (4% NaCl) flowing (crossflow) on the shell side at an inlet temperature of 90°C (tube side: D.I. water, inlet temperature 33-35°C, linear velocity 4250 cm/min)

FIG. 10

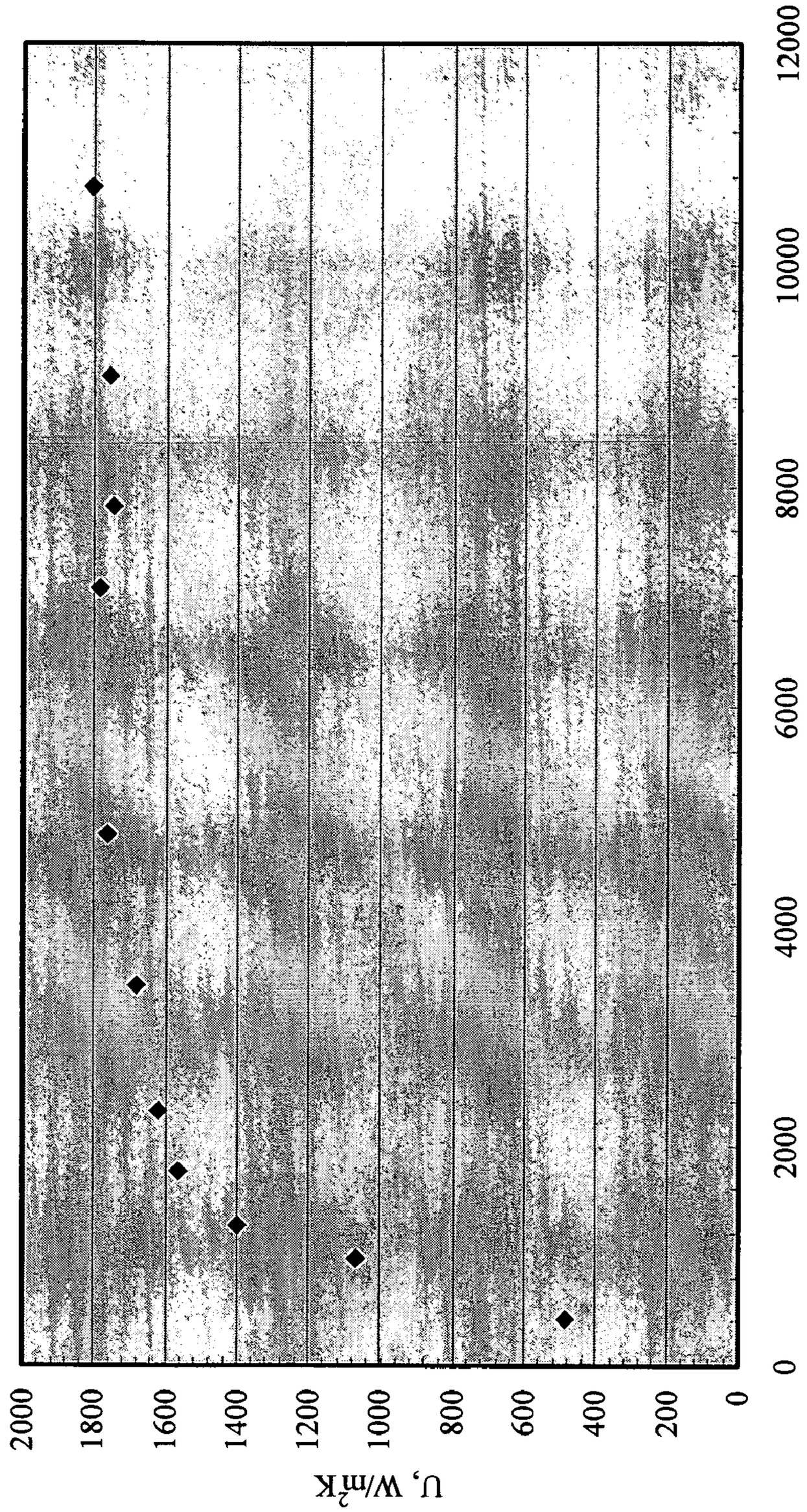

Variation of overall heat transfer coefficient of membrane module HEPP1 (containing 79 PP fibers having I.D. 0.0425 cm, O.D.0.0575 cm and I.D. surface area 195 cm^2) with linear velocity of cooling water (D.I. water) on the tube side at an inlet temperature of 30-45°C (shell side: 4% NaCl, inlet temperature of 90°C, interstitial velocity 254 cm/min, crossflow)

FIG. 11

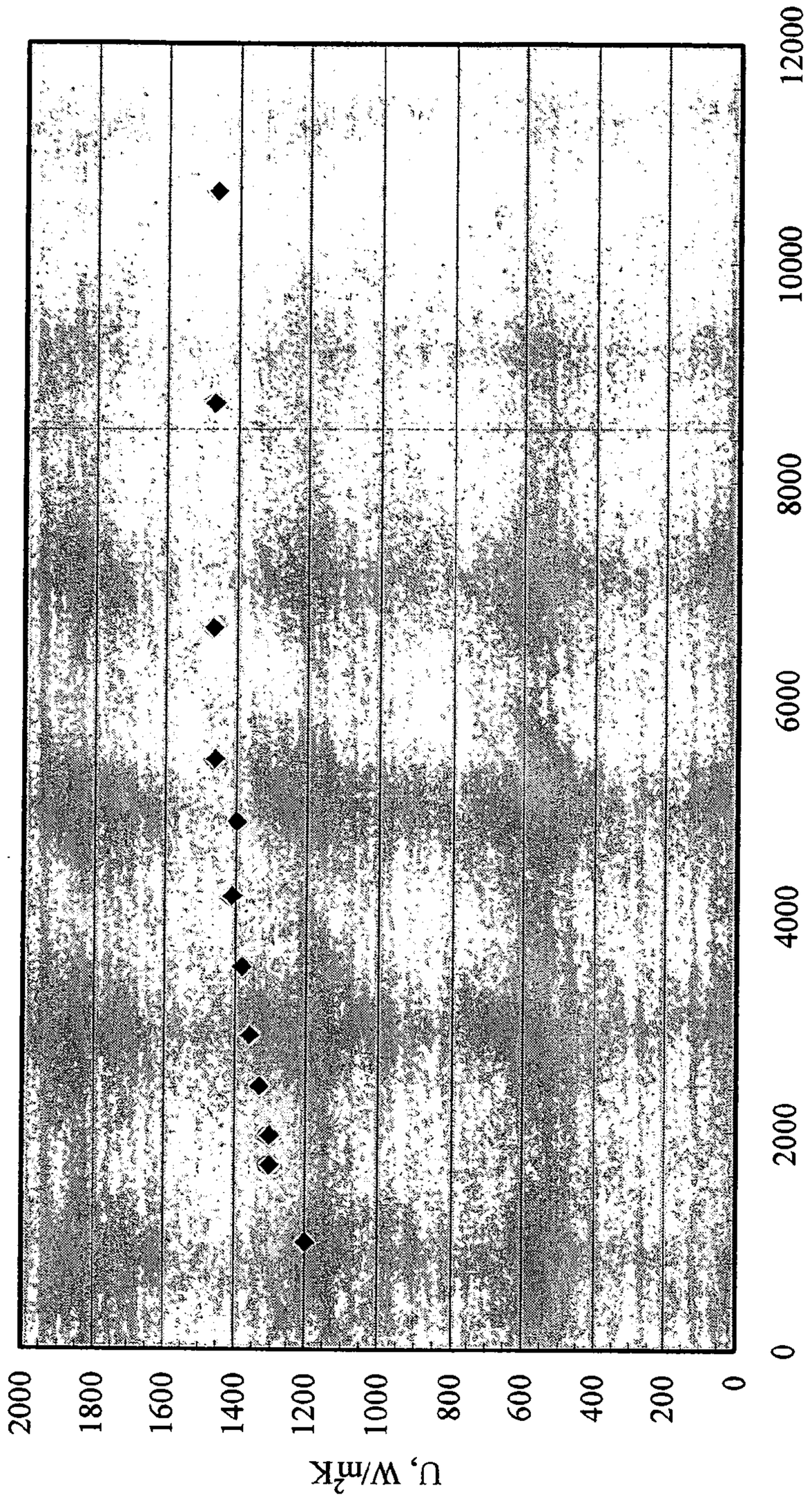

Variation of overall heat transfer coefficient of membrane module HEPP1 (containing 79 PP fibers having I.D. 0.0425 cm, O.D. 0.0575 cm and I.D. membrane surface area 195 cm^2) with linear velocity of hot brine (4% NaCl) flowing on the tube side at an inlet temperature of 90°C (shell side: D.I. water, inlet temperature 33-41°C, interstitial velocity 258 cm/min, crossflow)

FIG. 12

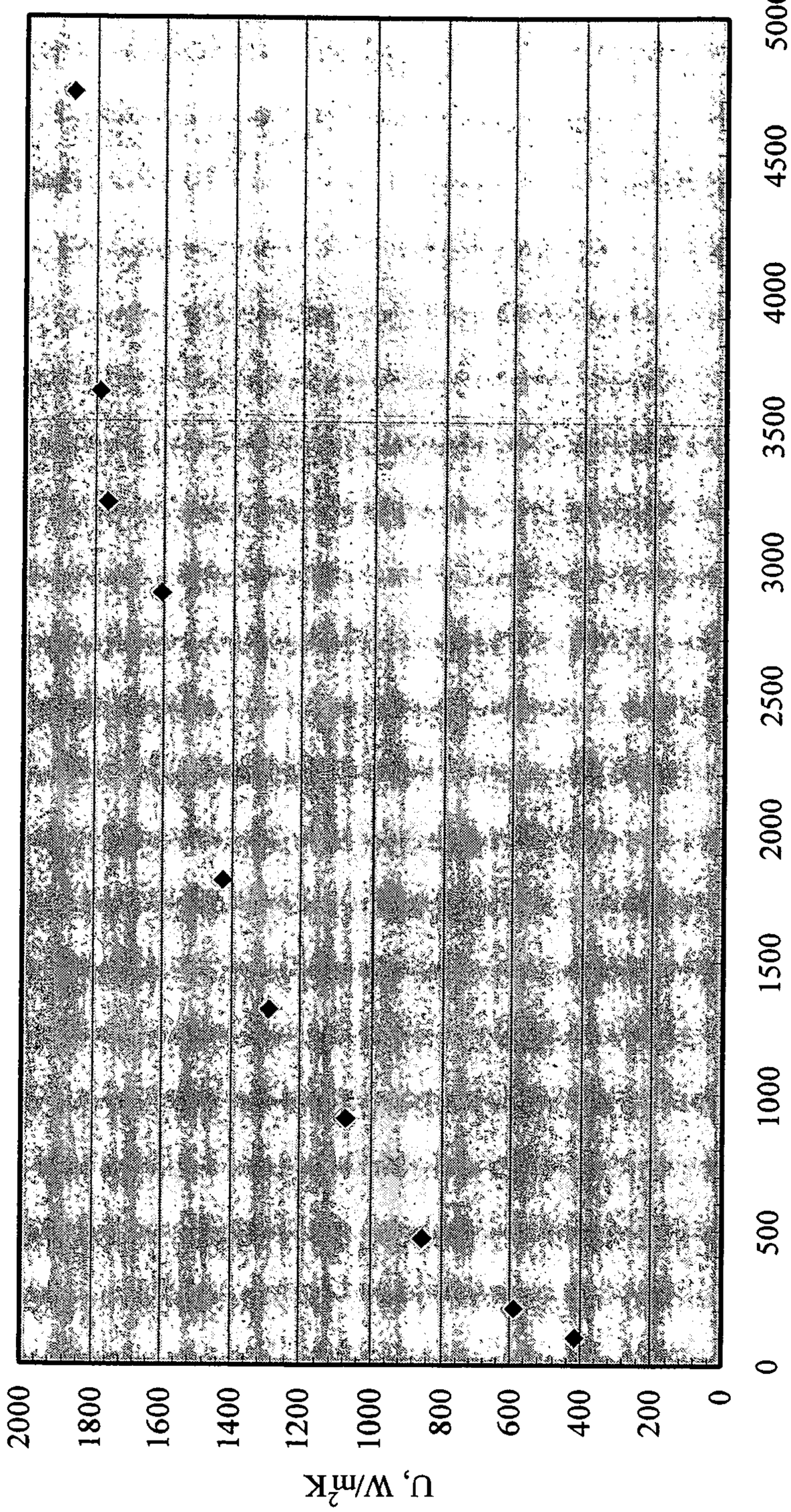

Variation of overall heat transfer coefficient of membrane module HEPP1 (containing 79 PP fibers having I.D. 0.0425 cm, O.D. 0.0575 cm and I.D. surface area 195 cm^2) with linear velocity of hot brine (4% NaCl) flowing (parallel) on the shell side at an inlet temperature of 90°C (tube side: D.I. water, inlet temperature 33-38°C, linear velocity 4250 cm/min)

FIG. 13

Variation of overall heat transfer coefficient of membrane module **HEPEEK1** (containing 50 PEEK fibers having I.D. 0.015 cm, O.D. 0.036 cm and I.D. surface area 54.2 cm^2) with interstitial velocity of hot brine (4% NaCl) flowing (crossflow) on the shell side at an inlet temperature of 90°C (tube side: D.I. water, inlet temperature 27-30°C, linear velocity 3830 cm/min)

FIG. 14

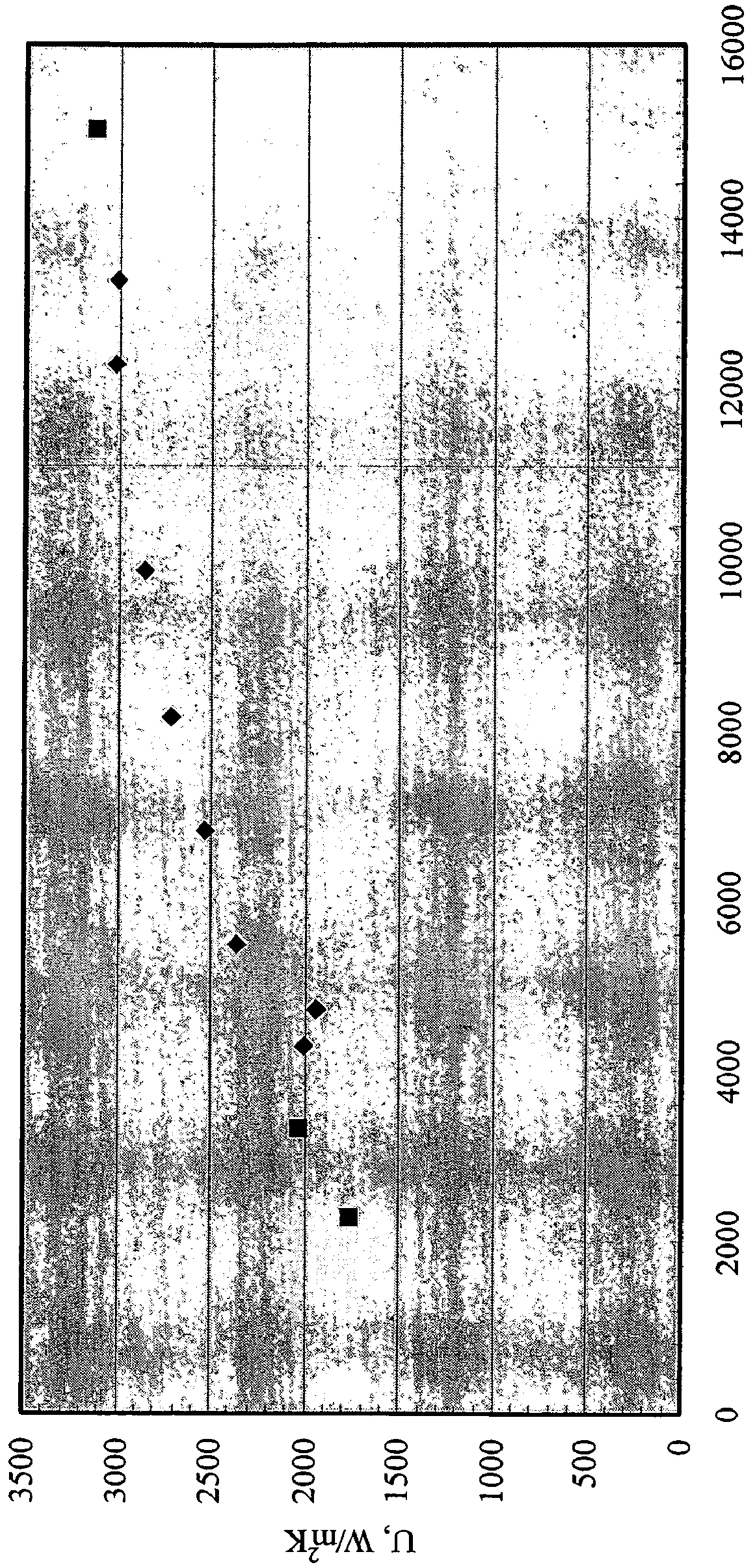

Variation of overall heat transfer coefficient of membrane module HEPES1 (containing 8 coated porous asymmetric UltraPES fibers having I.D. 0.07 cm, O.D. 0.1 cm and I.D. surface area 26.4 cm^2) with linear velocity of hot brine (4% NaCl) flowing on the tube side at an inlet temperature of 90°C (shell side: D.I. water, inlet temperature 20° C linear flow rate 3600 cm/min); interfacially polymerized nonporous coating on I.D.

FIG. 15

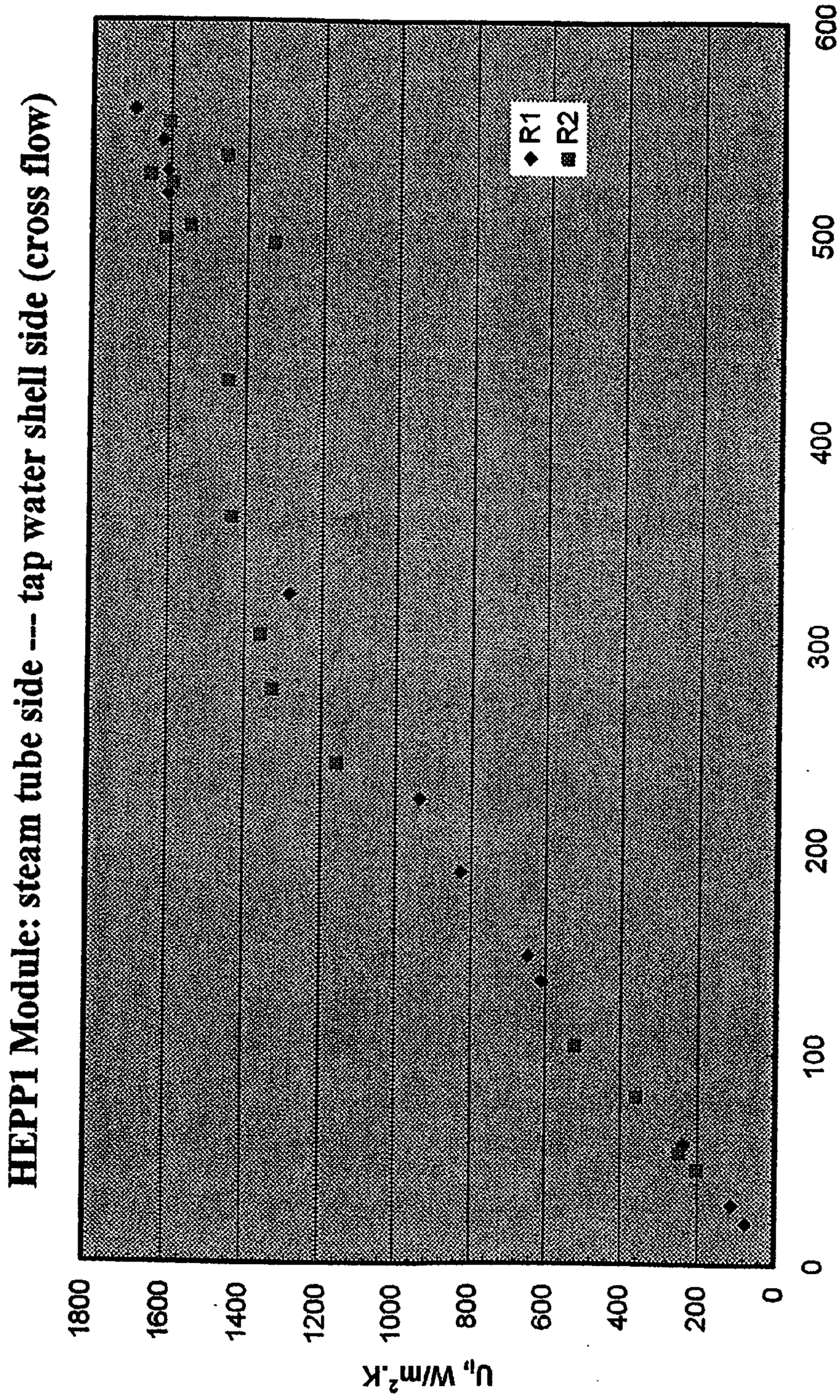

FIG. 16

Variation of overall heat transfer coefficient of module HEPP1 with linear velocity of steam flowing on the tube side at an inlet temperature between 101-113° C (Re_t: 3-100) (shell side: tap water, cross flow, inlet temperature 20°C, interstitial velocity 300 cm/min, Re_s: 26-31)

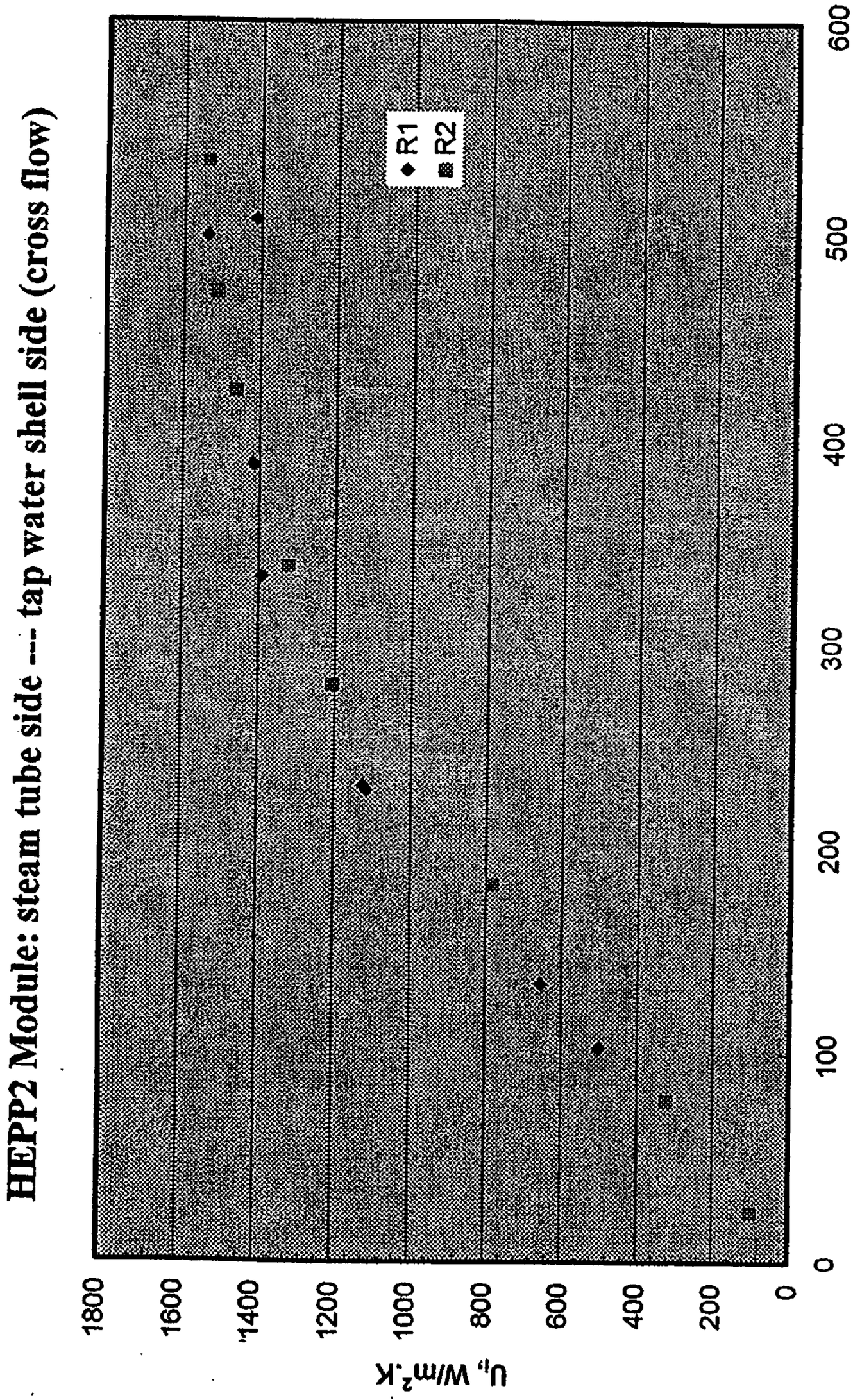

Variation of overall heat transfer coefficient of module HEPP2 with linear velocity of steam flowing on the tube side at an inlet temperature between 103-113°C (Re_t: 15-105) (shell side: tap water, **cross flow**, inlet temperature 16.7°C, interstitial velocity 860 cm/min, Re_s: 79-90)

FIG. 17

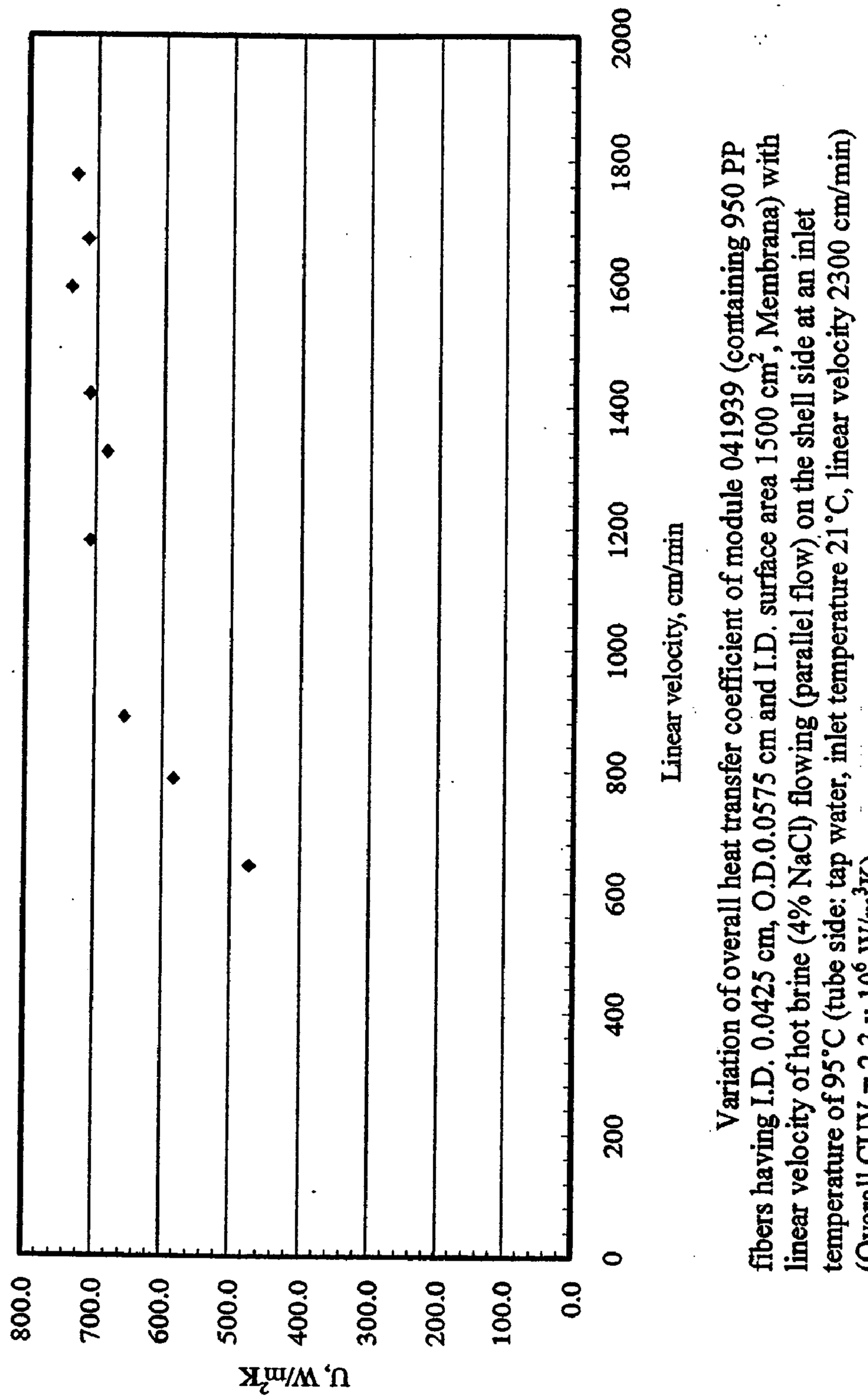

Variation of overall heat transfer coefficient of module 04193 (containing 950 PP fibers having I.D. 0.0425 cm, O.D.0.0575 cm and I.D. surface area 1500 cm^2, Membrana) with linear velocity of hot brine (4% NaCl) flowing (parallel flow) on the shell side at an inlet temperature of 95°C (tube side: tap water, inlet temperature 21°C, linear velocity 2300 cm/min) (Overall CUV = 2.3 x 10^6 W/m^3K).

FIG. 18

Particulars	HEPP1	HEPP2	HEPP3	HEPES3	HEPEEK2
Support hollow fiber type (thickness/I.D., μm)	PP 75/425			PES 150/700	PEEK 75/420
Support material	PP			PES	PEEK
Fiber O.D., μm	575			1000	570
Fiber I.D., μm	425			700	420
Wall thickness, μm	75			150	75
Pore size (μm or MWCO)	-	-	-	70,000	-
Membrane porosity, %	-	-	-	-	-
Coating	-	-	-	Nonporous	-
No. of fiber	79	400	200	6	79
Effective fiber length, cm	18.5	18.0	21.5	23.5	18.5
Actual fiber length inside the module, cm	25.0	27.5	28.5		26.7
Effective fiber surface area(ID)*, cm^2	195.0	960.8	573.8	31.0	192.7
Fiber surface area/volume*, m^2/m^3	531	1404	1345	730	537
Arrangement of fiber	Matted			Not matted	
Effective cross-section area for shell side liquid flow**, cm^2	15.5	17.51	21.27	0.134	15.9
Shell side tubing material	PP			PTFE	PP
Shell side tube I.D., cm	1.59	2.20	1.59	0.48	1.59
Shell side tube O.D., cm	1.91	2.54	1.91	0.95	1.91
Distribution tube I.D., cm	0.48	0.60	0.48	-	0.48
Distribution tube O.D., cm	0.79	0.95	0.79	-	0.79
Packing fraction of fibers	0.137	0.247	0.18	0.128	0.135
Shell side flow mode	Cross/parallel flow			Parallel flow	Cross/parallel flow
Fabricated at	New Jersey Institute of Technology				

* Based on fiber internal diameter

** Based on open area for flow = total cross sectional area – fiber projected area.

FIG. 19

Particulars	HEPEEK1	HEPES1
Support membrane type	PEEK 105/150	PES 150/700
Support membrane	PEEK	PES
Fiber O.D., μm	360	1000
Fiber I.D., μm	150	700
Wall thickness, μm	105	150
Maximum pore size, μm	--	
Membrane porosity, %	--	
Coating	--	Polyamide
No. of fibers	50	8
Effective fiber length, cm	23	15
Effective membrane surface area (ID)*, cm^2	54.2	26.38
Membrane surface area/volume, m^2/m^3	70	970
Effective cross-sectional area for shell side liquid flow**, cm^2	30.8	0.254
Module frame (internal dimensions)	Shell Material: PP; ID: 1.59cm	Shell Material: PTFE; ID: 0.48 cm
Packing fraction of fibers	0.034	0.118
Shell side flow mode	Cross/parallel flow	Parallel flow
Fabricated at	New Jersey Institute of Technology	

* Based on fiber internal diameter.
** Based on open area for flow = total cross sectional area – fiber projected area.

FIG. 19
Cont'd

Particulars	#041938	#041938	#041941
Support fiber type (wall thickness/I.D., μm)	PP 75/430		
Support material	PP		
Fiber O.D., μm	580		
Fiber I.D., μm	430		
Wall thickness, μm	75		
No. of fibers	950		2750
Effective fiber length, cm	11.8		11.8
Effective fiber surface area(ID)*, m^2	0.15		0.44
Fiber surface area/volume*, m^2/m^3	3061		3290
Arrangement of fiber	matted		
Shell side tube I.D., cm	2.3		3.8
Packing fraction	0.59		0.63
Shell side material	Polycarbonate housing		
Shell side flow mode	Parallel flow		
Fabricated at	Membrana-Charlotte, NC		

* Based on fiber internal diameter

FIG. 20

Exp	T_{t1} (°C)	T_{t2} (°C)	T_{s1} (°C)	T_{s2} (°C)	T_s(av) (°C)	F_t (ml/min)	T_t(av.) (°C)	T_{t2}-T_{t1} (°C)	A (I.D.m^2)	Q(I.D.) W/M^2	T_s-T_t (°C)LN	U W/M^2K
Exp. No. 1	28.5	86.4	90.0	88.8	89.4	47.0	57.5	57.9	0.0195	9722.3	20.1	483.3
Exp. No. 2	29.3	86.6	90.8	89.0	89.9	109.0	58.0	57.3	0.0195	22313.7	20.9	1067.1
Exp. No. 3	29.5	85.9	90.0	87.8	88.9	142.0	57.7	56.4	0.0195	28612.6	20.4	1401.4
Exp. No. 4	29.8	83.5	90.5	87.8	89.2	197.0	56.7	53.7	0.0195	37794.7	24.1	1567.0
Exp. No. 5	30.2	79.0	90.0	86.9	88.5	259.0	54.6	48.8	0.0195	45155.4	27.9	1620.3
Exp. No. 6	33.4	72.3	89.9	86.0	88.0	387.0	52.9	38.9	0.0195	53783.7	32.0	1682.4
Exp. No. 7	36.2	67.1	89.4	85.2	87.3	542.0	51.7	30.9	0.0195	59834.0	33.9	1764.2
Exp. No. 8	41.0	63.4	90.8	86.2	88.5	793.0	52.2	22.4	0.0195	63461.7	35.6	1784.6
Exp. No. 9	40.9	61.4	90.8	86.0	88.4	876.0	51.2	20.5	0.0195	64157.6	36.7	1748.6
Exp. No. 10	45.0	59.8	90.1	85.5	87.8	1200.0	52.4	14.8	0.0195	63450.3	35.2	1804.9
Exp. No. 11	45.7	62.2	90.3	85.9	88.1	1008.0	54.0	16.5	0.0195	59420.3	33.8	1758.5

FIG. 21

Module	α **	U_i***	CUV_i	HTU	NTU	ε ****
	m^2/m^3	$W/m^2.K$	$W/m^3.K$	cm		
HEPP1	531	450-1936	$2.4x10^5$-$1x10^6$	6.0-43.4	0.35-3.12	0.17-1
HEPP2	1404	505-2076	$7.1x10^5$-$2.9x10^6$	4.6-66.7	0.27-3.91	0.19-1
HEPP3	1345	319-1799	$4.3x10^5$-$2.4x10^6$	8.0-91.0	0.27-2.69	0.14-1
HEPEEK2	537	535-1929	$2.8x10^5$-$1.0x10^6$	14-106	0.17-2.66	0.14-0.89
Membrana	3061	211-1100	$6.1x10^5$-3.5×10^6	4.6-21.7	0.54-2.59	0.35-0.89
HEPES3	730	804-2109	$5.9x10^5$-1.5×10^6	16-135.5	0.2-1.5	0.15-0.77

* hot brine and water; ** surface area/volume; *** overall heat transfer coefficient; **** heat exchanger effectiveness

FIG. 22

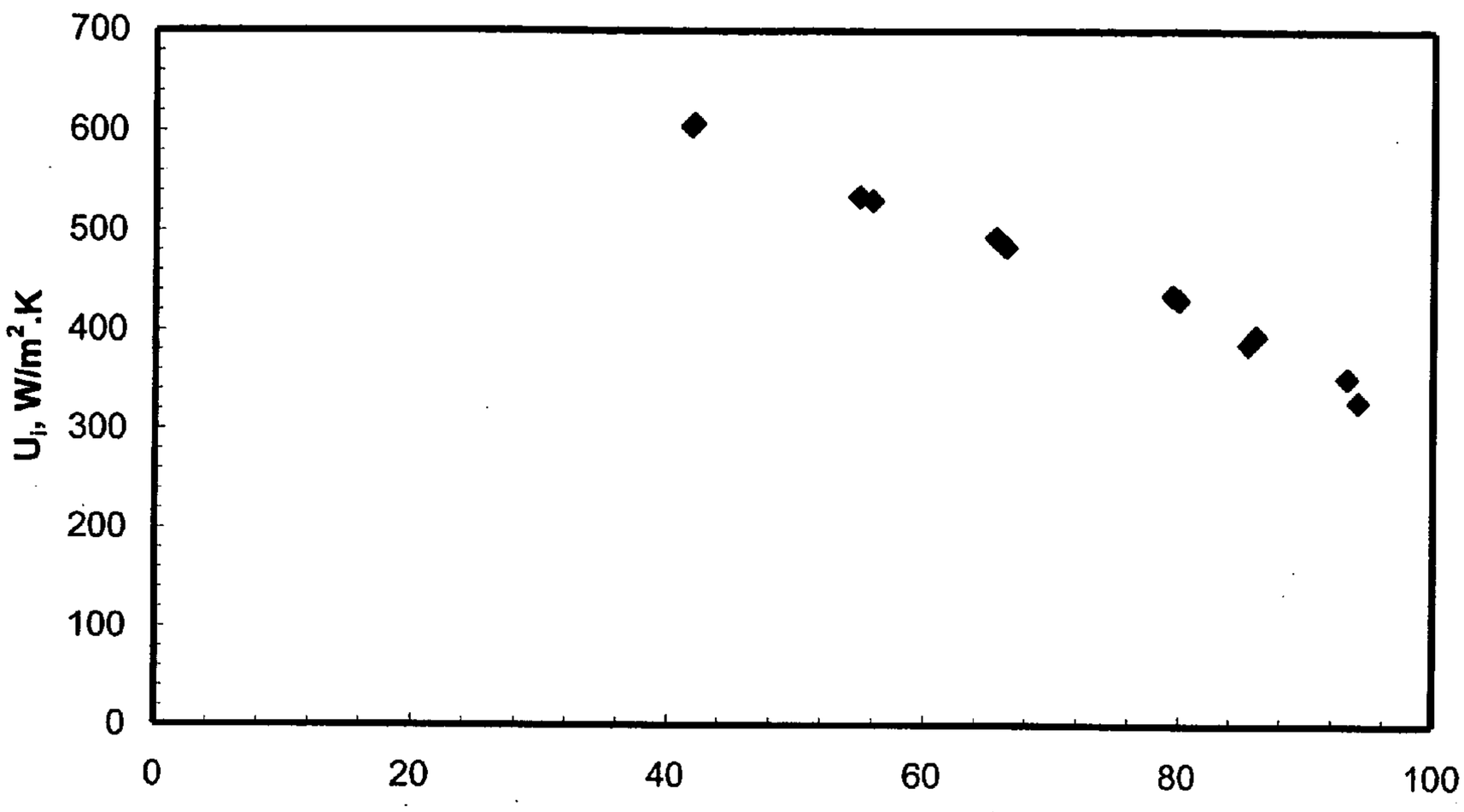

Variation of heat transfer coefficient of module HEPP4 with feed temperature of hot brine flowing on the tube side at a flow rate 20 L/min (Shell side: city water, flow rate 11.3 L/min, temperature 21.3 - 22.3 °C)

FIG. 23

POLYMERIC HOLLOW FIBER HEAT EXCHANGE SYSTEMS

CROSS-REFERENCE TO RELATED APPLICATION(S)

[0001] The present application claims the benefit of a co-pending provisional patent application entitled "Polymeric Hollow Fiber Heat Exchange Systems," which was filed on Oct. 27, 2005 and assigned Ser. No. 60/730,954. The entire contents of the foregoing provisional patent application are incorporated herein by reference.

BACKGROUND

[0002] 1. Technical Field

[0003] The present disclosure is directed to advantageous heat exchange systems that include one or more polymeric solid hollow fibers and, more particularly, asymmetric porous hollow fiber-based heat exchange systems that provide enhanced heat transfer in a variety of applications, e.g., desalination applications, solar heating applications, applications in the chemical industry, and/or applications in the biotechnology, biomedical or pharmaceutical industry. Exemplary embodiments of the disclosed heat exchange systems are characterized by hollow fibers that include a microporous wall and a dense skin formed thereon, thereby preventing liquid transmission and/or contamination through the wall of the hollow fiber while simultaneously enhancing heat transfer based on the presence of liquid molecules within the porous substructure of the hollow fiber. The disclosed hollow fiber systems may be advantageously employed with a variety of heat exchange applications, including aqueous/aqueous heat exchange systems, aqueous/steam heat exchange systems, steam/organic solvent heat exchange systems, and aqueous/organic solvent heat exchange systems.

[0004] 2. Background Art

[0005] It is known that polymeric materials offer numerous advantages over metals in the construction of heat exchange systems, e.g., reduced cost, ease of fabrication and lower weight. In addition, from an energy requirements standpoint, the fabrication of polymeric materials involves energy input that is reduced by a factor of two relative to common metals. Moreover, the surface of plastics is generally smooth, which translates to: (1) less fouling than metal tubes, and (2) potentially smaller friction forces and pressure drops. As a general matter, plastics possess excellent chemical resistance to acids, oxidizing agents, and many solvents.

[0006] Despite the advantages associated with polymeric materials for the fabrication of heat exchange systems, disadvantages remain. In particular, polymeric materials exhibit low thermal conductivity relative to metals, thereby significantly reducing their utility in heat transfer applications. For example, polymeric materials generally exhibit thermal conductivity in the range of 0.1 to 0.4 W/m° K., which is 100-300 times lower than that of metals. Thus, the commercial and/or industrial utility of polymeric heat exchange systems has been limited.

[0007] Conventional use of large-scale metallic tubes in condensers and heat exchangers employed in multi-stage flash, multiple effect and vapor compression distillation-based desalination processes has led to huge capital investments, excessive corrosion/erosion of the tubes in the presence of hot brine, heavy metal contamination of waste brine, relatively large footprints, and excessive weight. Thus, the elimination/replacement of conventional metallic tube condensers and heat exchangers with polymeric hollow fiber heat exchange systems that provide effective heat transfer performance would be highly desirable.

[0008] The patent literature includes teachings with respect to polymer-based hollow fiber membranes. Exemplary teachings include:

[0009] Knickel, U.S. Pat. No. 4,036,748, which discloses asymmetric semi-permeable membranes for desalination that can be produced from solution in the form of hollow fibers.

[0010] Leonard, U.S. Pat. No. 3,724,672, which describes a "skin-core structure."

[0011] Semmens, U.S. Pat. No. 4,960,520, which discloses hollow fiber membranes of microporous polypropylene with a very thin outside coating of plasma polymerized disiloxane. The fibers are potted in a module which resembles a shell and tube heat exchanger. Strippant is pumped through the shell side of the module and over the outside of the fibers. The volatile and semi-volatile contaminants in the water diffuse across the membrane and dissolve into the oil. The process results in clean water and a smaller volume of more highly contaminated oil.

[0012] Beyond the foregoing U.S. patents, two Japanese patent abstracts are noted that discuss the use of polymeric hollow fibers for heat transfer. Matsuro Suzuki, Japanese Patent No 60200097, discusses hollow fibers molded of heterogeneous film (polyphenylene sulfide) to increase thermal efficiency of a heat exchanger. Eiichi Hamade, Japanese Patent No 61083898, discusses heat transfer of water, organic liquid or gaseous bodies by hollow fibers.

[0013] The prior art also includes teachings with respect to systems that include polymeric hollow fibers for heat transfer in aqueous systems. For example, U.S. Pat. No. 5,863,654 to Frey discloses a biocompatible porous hollow fiber made of a polyolefin material that includes a coating of biocompatible carbon material. Frey discloses that the foregoing hollow fibers may be used in heat exchange devices, e.g., within oxygenators. U.S. Pat. No. 5,876,667 to Gremel discloses a heat exchanger of polymeric hollow fibers with a wetting agent coating.

[0014] Zaheed et al. discuss the performance characteristics and uses of a cross-corrugated, polymer film, compact heat-exchanger (PFCHE) made of polyetheretherketone (PEEK) in aqueous-aqueous systems. Zaheed, L., Jachuck, R. J. L., *Performance of a Square, Cross-Corrugated, Polymer Film, Compact, Heat-Exchanger with Potential Application in Fuel Cells, Journal of Power Sources*, v. 140 (2005), pp 304-310. Konagaya discusses hollow fiber configurations for use in reverse osmosis applications consisting of a top skin, dense layer, and a microporous layer. Konagaya, S., *New Chlorine-Resistant Polyamide Reverse Osmosis Membrane with Hollow Fiber Configuration, Journal of Applied Polymer Science*, v. 79 (2001) 517 et seq.

[0015] Despite efforts to date, a need remains for polymeric heat exchange systems that offer enhanced heat trans-

fer performance. In addition, processing designs and systems utilizing polymeric heat exchange elements for effecting heat exchange with steam, e.g., low temperature steam, are needed. These and other needs are satisfied by the heat exchange systems disclosed herein.

SUMMARY OF THE DISCLOSURE

[0016] The present disclosure provides advantageous heat exchange systems that include one or more asymmetric polymeric solid hollow fibers. Exemplary asymmetric polymeric solid hollow fibers according to the present disclosure are characterized by hollow fibers that include a microporous wall and a dense skin formed thereon, thereby preventing liquid transmission and/or contamination through the wall of the hollow fiber while simultaneously enhancing heat transfer based on the presence of liquid molecules within the porous substructure of the hollow fiber. The disclosed asymmetric hollow fibers may be employed in a variety of heat transfer-related commercial/industrial applications, including desalination applications, solar heating applications, applications in the chemical industry, and applications in the biotechnology or pharmaceutical industry. For example, the disclosed asymmetric polymeric solid hollow fibers may find advantageous application in extracorporeal blood oxygenation systems with the heat exchange fluid on the porous wall side.

[0017] In addition, the present disclosure provides heat transfer systems wherein steam is advantageously condensed on a first side of a polymeric, hollow fiber-based heat exchanger. The condensed steam provides energy that may be used to heat water and/or other liquids that flow on a second side of the polymeric, hollow fibers. Indeed, by using a steam feed that is adapted to condense on one side of the hollow fibers (rather than a gas) and a liquid on the other side, overall heat transfer coefficients on the order of a liquid-liquid heat exchanger can be achieved with the disclosed heat transfer system (if not higher). According to exemplary embodiments of the disclosed steam condensation heat transfer systems, a hydrophobic polymeric surface (e.g., polypropylene) may effect drop-wise condensation of the steam, thereby enhancing the overall heat transfer performance of the disclosed systems. Condensation of the steam is generally effected to form relatively small droplet sizes, thereby minimizing the likelihood of condensation-related flow restriction on the steam side of the hollow fiber system.

[0018] Of note, the disclosed polymeric hollow fibers offer numerous industrial advantages. For example, the polymeric hollow fibers disclosed herein are substantially inert to a wide range of processing fluids/systems, e.g., brine-to-brine, brine-to-water, and steam-to-brine desalination applications. The polymeric hollow fibers are not susceptible to corrosion and/or erosion (which can limit the utility of metal heat exchange tubes), and may be fabricated in highly compact designs. Highly compact designs are feasible, at least in part, because the disclosed polymeric hollow fibers have a very high surface area per unit equipment volume (as compared to non-polymeric heat exchange systems or even other plastic heat exchange systems). Thus, an equivalent volume may be an order of magnitude smaller, thereby drastically reducing the associated system weight, footprint and cost.

[0019] Indeed, polymeric hollow fibers fabricated from such exemplary polymeric systems as polypropylene, polyethersulfone (PES), polyetheretherketone (PEEK), polyimides, polyphenylene sulfide (PPS), polyethylene (PE), polytetrafluoroethylene (PTFE), polysulfone (PS), poly-4-methyl-1-pentene (PMP) and the like, are generally unaffected by hot brine, cold brine, pH values over a wide range, a host of chemical systems, and a host of solvents. The disclosed polymeric hollow fibers may be advantageously employed in a variety of organic-aqueous and organic-organic heat transfer systems, provided the polymeric material provides suitable levels of stability with the organic molecules to be processed.

[0020] Additional advantageous features and functions of the disclosed heat exchange systems and associated heat exchange processes will be apparent from the detailed description which follows, particularly when read in conjunction with the appended figures.

BRIEF DESCRIPTION OF THE FIGURES

[0021] To assist those of skill in the art in making and using the disclosed heat exchange systems, reference is made to the accompanying figures, wherein:

[0022] FIG. **1** is a plan view of an exemplary cross/parallel flow module employed in experimental work according to the present disclosure;

[0023] FIG. **2** is a plan view of a further exemplary cross/parallel flow module according to the present disclosure;

[0024] FIG. **3** is a plan view of an additional cross/parallel flow module according to the present disclosure;

[0025] FIG. **4** is a plan view of a plurality of modules according to the present disclosure;

[0026] FIG. **5** provides a schematic cross-sectional diagram of a cross/parallel flow module with flow direction at the shell side utilized in the experimental work described herein;

[0027] FIG. **6** is a schematic diagram of an experimental system used in measuring heat exchange performance according to the present disclosure;

[0028] FIG. **7** is a schematic diagram of an experimental setup for membrane gas permeation measurements according to the present disclosure;

[0029] FIG. **8***a* is a temperature profile plot in solid hollow fiber heat exchangers for a hot brine-cold water/brine system;

[0030] FIG. **8***b* is a temperature profile plot in solid hollow fiber heat exchangers for a steam-cold water/brine system;

[0031] FIG. **9** is a plot of overall heat transfer coefficient (U) of module HEPP**1** relative to feed inlet temperature obtained through experimental studies according to the present disclosure;

[0032] FIG. **10** is a plot of overall heat transfer coefficient (U) of module HEPP**1** relative to interstitial velocity of hot brine flowing on the shell side in crossflow, obtained through experimental studies according to the present disclosure;

[0033] FIG. **11** is a plot of overall heat transfer coefficient (U) of module HEPP**1** relative to linear velocity of cooling

water flowing on the tube side with brine on shell side in crossflow, obtained through experimental studies according to the present disclosure;

[0034] FIG. **12** is a plot of overall heat transfer coefficient (U) of module HEPP**1** relative to linear velocity of hot brine flowing on the tube side with D.I. water flowing in shell side in crossflow, obtained through experimental studies according to the present disclosure;

[0035] FIG. **13** is a plot of overall heat transfer coefficient (U) of module HEPP**1** relative to linear velocity of hot brine flowing on the shell side in parallel flow, obtained through experimental studies according to the present disclosure;

[0036] FIG. **14** is a plot of overall heat transfer coefficient (U) of module HEPEEK**1** relative to interstitial velocity of hot brine flowing on the shell side in crossflow, obtained through experimental studies according to the present disclosure;

[0037] FIG. **15** is a plot of overall heat transfer coefficient (U) of module HEPES**1** relative to linear velocity of hot brine flowing on the tube side and D.I. water flowing on the shell side in parallel flow, obtained through experimental studies according to the present disclosure;

[0038] FIG. **16** is a plot of overall heat transfer coefficient (U) of module HEPP**1** relative to linear velocity of steam flowing on the tube side and tap water flowing on the shell side in cross flow, obtained through experimental studies according to the present disclosure;

[0039] FIG. **17** is a plot of overall heat transfer coefficient (U) of module HEPP**2** relative to linear velocity of steam condensing on the tube side and tap water flowing on the shell side in cross flow, obtained through experimental studies according to the present disclosure;

[0040] FIG. **18** is a plot of overall heat transfer coefficient (U) of a large module 041939 relative to linear velocity of hot brine flowing on the shell side in parallel flow with tap water in tube side flow, obtained through experimental studies according to the present disclosure;

[0041] FIG. **19** is a table setting forth design details with respect to modules fabricated at NJIT;

[0042] FIG. **20** is a table setting forth design details with respect to solid hollow fiber modules obtained from Membrana (Charlotte, N.C.);

[0043] FIG. **21** is a table setting forth experimental data for experimental runs using module HEPP**1** according to the present disclosure;

[0044] FIG. **22** is a table setting forth solid hollow fiber heat exchanger performance data for hollow fiber systems with hot brine/water according to the present disclosure; and

[0045] FIG. **23** is a plot of heat transfer coefficient relative to temperature for an exemplary solid hollow fiber exchanger (HEPP**4**) according to the present disclosure.

DESCRIPTION OF EXEMPLARY EMBODIMENT(S)

[0046] As noted above, the present disclosure provides advantageous heat exchange systems that include one or more polymeric solid hollow fibers and, more particularly, asymmetric porous hollow fiber heat exchange systems that provide enhanced heat transfer in a variety of applications, e.g., desalination applications, solar heating applications, applications in the chemical industry, applications in the biomedical industry and/or applications in the biotechnology industry. Exemplary embodiments of the disclosed heat exchange systems are characterized by hollow fibers that include a microporous wall and a dense skin formed thereon, thereby preventing liquid transmission and/or contamination through the wall of the hollow fiber while simultaneously enhancing heat transfer based on the presence of liquid molecules within the porous substructure of the hollow fiber. The disclosed heat exchange systems advantageously provide improved processing performance and reduced cost for industrially significant processing schemes, e.g., thermally-driven desalination processes, by employing thermally, chemically and mechanically stable polymeric solid hollow fibers with an ultrathin wall.

[0047] Exemplary heat exchange systems according to the present disclosure are described in greater detail below, with particular reference to experimental studies associated therewith. As described herein, compact and lightweight devices for heat exchange are provided. The heat transfer characteristics of such devices for steam-brine and water-brine heat exchange have been studied and experimental reports reported below. As demonstrated by such experimental results, advantageous modifications to asymmetric hollow fibers have been undertaken so as to achieve improved/enhanced heat exchange performance. The disclosed polymeric solid, hollow fibers are chemically inert, environmentally benign and have strong, but ultrathin, walls (e.g., about 40-100 μm thickness), which yield advantageous and industrially acceptable wall heat transfer coefficient values.

Technical Approach to Experimental Studies

[0048] Step 1: Procure solid hollow fibers fabricated from a variety of polymers.

[0049] Step 2: Fabricate small heat exchanger modules of 20-50 cm length containing 200-400 solid hollow fibers (see Step 1) and procure solid hollow fiber modules of larger surface area.

[0050] Step 3: Develop setup(s) to study heat exchange between steam and brine, hot brine and cold brine, and hot brine and cold water.

[0051] Step 4: Determine the overall heat transfer coefficients achieved in the smaller heat exchange modules (see Step 2) for steam-cold brine as well as hot brine-cold water heat exchange.

[0052] Step 5: Measure the moisture permeance of selected polymeric hollow fibers.

[0053] Step 6: Make a preliminary heat transfer coefficient measurement in the hollow fiber module having a larger surface area.

Experimental Details

[0054] 1. Initial Experimental Modules

[0055] Three cross flow modules of solid polypropylene (PP) hollow fibers, two cross flow modules of solid polyetheretherketone (PEEK) hollow fibers, and two parallel flow modules of asymmetric polyethersulfone (UltraPES) hollow fibers were fabricated in a laboratory at New Jersey

Institute of Technology (Newark, N.J.); three large parallel flow modules of solid PP hollow fibers were obtained from Membrana GmbH (Charlotte, N.C.). Dense PP hollow fibers having a solid wall thickness of 75 μm and outer diameter (OD) of 575 μm used in the NJIT modules and Membrana modules (described below) were obtained from Membrana; the dense PEEK hollow fibers were obtained from Upchurch Scientific, Inc. (Oak Harbor, Wash.) and the porous UltraPES hollow fibers were also obtained from Membrana. The porous UltraPES hollow fibers were coated with a nonporous polyamide film on the internal diameter of the fibers by interfacial polymerization performed in the NJIT laboratories. The coating system and procedure are described below.

[0056] The interfacial polycondensation reaction of

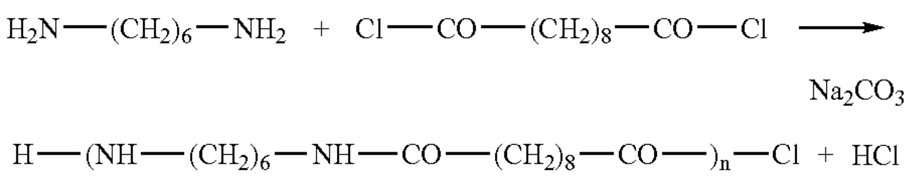

was carried out using the following system:

[0057] Aqueous solution: 1% 1,6-Hexanediamine

[0058] Organic solution: 1% Sebacoyl chloride in Xylene

[0059] Alkaline agent to remove HCl formed: Na_2CO_3

[0060] Reaction time: 2 minutes at room temperature

[0061] Number of coatings: 3

[0062] The exemplary coating procedure performed according to the present disclosure involved the following steps: Fiber pores were wetted with the aqueous monomer (hexanediamine) solution and the organic solution having monomer (sebacoyl chloride) was passed through the lumen side of the fibers to form an interfacially polymerized polyamide film on the inner diameter (ID) of the fibers.

[0063] According to further exemplary embodiments of the present disclosure, the internal surfaces of the disclosed fibers have been provided with an advantageous bilayer coating. In an exemplary bilayer coating process with respect to asymmetric PES (polyethersulfone) hollow fibers (e.g., UltraPES fibers; Membrana), a first coating layer is applied to the lumen side of the PES fibers by reacting an aqueous solution of a first reactant, e.g., 0.5% poly(ethyleneimine), and an organic solution of a second reactant, e.g., 0.5% iso-phthaloyl dichloride in xylene. Exemplary reaction conditions involve a reaction at room temperature for about ten (10) minutes, followed by heat treatment at an elevated temperature (e.g., about 100° C.) for about twenty (20) minutes. Thereafter, a second coating layer, e.g., a cross-linked polydimethylsiloxane (PDMS), is applied to the lumen side of the PES fibers. The PDMS coating may be applied to the disclosed PES fibers that already possess a first coating layer by introducing a silicone solution (e.g., 1% solution of silicone in hexane) and a curing agent at an appropriate concentration (e.g., 0.1%) to the fiber lumena and curing such second coating. Exemplary conditions include a first curing step in an oven at an elevated temperature, e.g., 110° C. for about forty (40) minutes, and a second cure at room temperature for an extended period, e.g., about two (2) days. The disclosed bilayer coating and comparable coating treatments may advantageously prevent and/or minimize any potential leakage through the fiber wall during heat exchange operations. The characteristics of the foregoing hollow fibers and the modules are listed in FIGS. **19** and **20**.

[0064] FIGS. **1-3** schematically depict exemplary modules fabricated at NJIT and utilized in the experimental studies described herein. Each of the test modules was fabricated to accommodate cross/parallel flow. With further reference to FIGS. **1-3**, exemplary modules were fabricated to include: (i) 79 polypropylene (PP) hollow fibers; (ii) 400 PP hollow fibers, (iii) 200 hollow fibers; (iv) 79 polyetheretherketone (PEEK) hollow fibers; and (v) 6 asymmetric ultra-polyethersulfone (UltraPES) fibers. Turning to FIG. **4**, a schematic depiction of three modules obtained from Membrana and used in the experimental work described herein is provided. The respective modules included: (i) 950 PP solid hollow fibers, and (ii) 2750 PP solid hollow fibers.

[0065] In order to maximize the brine-side boundary layer heat transfer coefficient on the shell side and investigate the effect of module flow configuration (parallel flow or cross flow) on the overall heat transfer coefficient, three PP-based and two PEEK-based cross/parallel flow modules were fabricated. A schematic diagram of the cross/parallel flow module is shown in FIG. **5**. The liquid entrance on the shell side of hollow fibers included a diverging section. The central feeder tube, with a wide size distribution of open holes, was fabricated using a PP tube. The hole distribution was implemented such that the holes near the entrance were smaller and those further out were larger. This hole distribution was adopted to ensure substantially uniform flow of the liquid (hot brine) in cross flow outside of and perpendicular to the hollow fibers, thereby providing effective heat transfer in the module. When liquid was introduced through the side entrance of module shell, parallel flow was obtained. The module shell consisted of a transparent PP tube having an appropriate thickness and heat transfer resistance.

[0066] 2. Experimental Apparatus and Procedures

[0067] The experimental apparatus employed in the experimental work described herein was developed such that the heat exchange process could be studied easily for small as well as large modules. A schematic diagram of the experimental system is set forth in FIG. **6**. The heat exchange module was assembled in heat transfer setups of differing size/scale—a smaller heat transfer setup and a corresponding experimental setup for larger modules.

[0068] In the smaller scale experimental setup, the system piping and storage tanks were thoroughly insulated to minimize heat loss to the environment. The liquids employed in the experiments were deionized (D.I.) water or tap water as cooling liquid and 4% (wt) solution of NaCl as feed solution. In the experimental procedure, the feed solution was introduced to the shell side/tube side from a hot brine reservoir by a digital Masterflex peristaltic pump at a constant flow rate. Two temperature controllers maintained the hot brine bath temperature at a given value and thus ensured the required temperature for the hot feed. Outside the module, the feed was circulated back to the feed reservoir and was rewarmed. Changes in shell side flow configuration (i.e.,

parallel flow versus cross flow) were implemented by switching to the corresponding liquid entrance as described above.

[0069] Deionized water or tap water was introduced as the cooling liquid on the fiber lumen side/shell side from a cooling bath by a second digital Masterflex peristaltic pump at a constant flow rate. The temperature of cooling liquid was maintained by a Cole-Parmer Polystat refrigerated bath (Model No. 12111-20) at a given low temperature before the water entered the module.

[0070] In the steam-water system, steam was generated by a steam generator having a heating capacity of 3 kW (Sussman Electric Boilers, Long Island City, N.Y.). The steam flow rate was controlled with a ball valve and measured by cooling down/condensing all steam flow into liquid. Steam was conducted from steam generator into the hollow fiber module using a thick wall polypropylene tubing. Before steam entered the module, the condensed water was trapped by a glass well. Normally solid wall PP cannot bear such high temperatures (around 120° C.). In the disclosed system, steam was passed through the tubing ID, while the outside surface of the tubing was exposed to air. The average temperature of the tubing was therefore maintained at a considerably lower level. The PP tubing worked well over the course of many experiments. The same conclusions proved valid for the stability of the dense PP hollow fibers in the test modules, since cold water was running on the other side (relative to steam within the fibers).

[0071] In the larger scale experimental setup for heat exchange operation, feed was introduced to the shell side of the larger module from a reservoir by a centrifugal pump (model: TE-4-MD-HC, Little Giant Co., Oklahoma City, Okla.) at a constant flow rate controlled by a ball valve. The flow rate of the liquid system could be varied between 5-40 liters per minute (LPM). Feed solution in a 200-liter stainless steel tank was heated by a heating system having two heaters (OMEGA, EMT-312E2/240 three-phase moisture resistant heater (12 kW); and EMT-309E2/240 three-phase moisture resistant heater (9 kW); total 21 kW heating capacity), two OMEGA rugged transition joint probes, two OMEGA three phase DIN rail mount solid state relays and two OMEGA CN77333 controllers. For safety, a liquid level switch was installed in the feed tank. Outside the module, the exiting feed was circulated back to the feed reservoir and was re-warmed. The steam generator used in this larger system had a heating capacity of 20 kW (Model # MBA2033 Sussman Electric Boilers, Long Island City, N.Y.).

[0072] The cooling system was mainly composed of a Remcor chiller having a cooling capacity of 12 kW (model: CH3002A, voltage (full load Amps): 230/60/3, IMI Cornelius Inc., Anoka, Minn.) with a recirculation pump and a 10 gallon tank. Deionized water was generally introduced as the cooling liquid on the fiber lumen side of the module from the reservoir at a constant flow rate. The exiting hot liquid stream from the module was cooled to a given temperature by the chiller before entering the module again. Tap water having a constant temperature (around 20° C.) was also used as an alternative source of cooling water on the tube side.

[0073] Each liquid solution (including the feed solution and the cooling water in the small scale system and the larger scale system) was filtered by passing through a post-filter cartridge (1 μm) (US Filter-Plymouth Products, Sheboygan, Wis.) before entering the module. The inlet and outlet temperatures of the hot feed solution/steam and the cold water were measured by four thermocouples with 0.1° C. accuracy. The pressure drops of the feed and the cold water through the module were also monitored. Conductivity meters (Model No. 115, Orion Research, Beverly, Mass.) were used to monitor potential leaks of the hollow fibers and/or the module. When the readings of the flow rates and temperatures reached constant values, it was assumed that a steady state had been reached. The steady inlet and outlet temperatures, pressures and the flow rates of the brine solution/steam and cold water were recorded for the calculation of heat exchange under the given experimental conditions.

[0074] Overall heat transfer coefficient, U, was calculated from the following relation:

$$U = \frac{F \times \rho \times \Delta t \times c_p}{s \times \Delta T_{\ell m}} \quad (1a)$$

where F: liquid stream flow rate; ρ: its density; Δt: liquid stream's inlet and outlet temperature difference; c_ρ: liquid stream heat capacity; ΔT_m: logarithmic mean bulk temperature difference between shell side and tube side (see equation 1b); s: hollow fiber surface area for heat transfer based on the inside area: $s=n\pi d_1 L$;

$$\Delta T_{\ell m} = \frac{(T_{s1} - T_{f2}) - (T_{s2} - T_{f1})}{\ell n\left[\frac{T_{s1} - T_{f2}}{T_{s2} - T_{f1}}\right]} \quad (1b)$$

Here T_{s1} and T_{s2} are the hot stream inlet and outlet temperatures and T_{f1} and T_{f2} are the cold stream inlet and outlet temperatures.

[0075] Leak testing: All modules listed in the tables of FIGS. **19** and **20** were tested for leakage before heat exchange measurements. Both exits of the tube side of module were connected to a N_2 cylinder; shell side openings were connected with an end of a thin tubing. The module was immersed into water. Gas pressure was slowly increased to 15 psi. Then the system was stabilized for 1 hr. If bubbles came from the shell side installed tubing, it indicated that the module was leaking; if there were no air bubbles, there was no leakage. The leakage was also measured by passing 4% NaCl solution through shell side at 8° C. or higher and 5 psi of inlet pressure; deionized water flowed through the tube side at room temperature. The conductivity of the deionized cold water was monitored with increasing brine pressure. If the conductivity of the distillate water rose with operating time, the test module was leaking. Otherwise, the module was leak free. The leak testing indicated that all modules listed in the tables of FIGS. **19** and **20** appeared to be in a good operational state under the test conditions.

[0076] Gas permeation: A system was also established for the measurement of gas permeance of the coated hollow fiber membranes using a gas permeation apparatus (FIG. **7**). The N_2 gas from the cylinder permeated through the membrane from the tube side to the shell side. The upstream and downstream pressures were measured by Ashcroft Test

Gauge (PT. No. 63-5631). The downstream flow rate of the gas was measured using a soap bubble flow meter. During the permeation measurements, the upstream pressure was maintained at a constant pressure, between 0.1-0.6 psig (0.5-3.1 cm Hg gauge). The permeation measurements were made at room temperature. As noted above, the permeant gas was N_2.

[0077] The N_2 permeance of the hollow fiber membranes is related to the measured steady-state permeation rate of nitrogen through the membrane by Eq. (2):

$$\frac{Q_{N_2}}{\delta_M}(\text{permeance}) = \frac{P_1 V_1 T_0}{P_0 T_1 \cdot s \cdot \Delta P_{N_2}} \quad (2)$$

In Eq. (2), T_0=273.15 K, P_0=760 Torr, ΔP_{N_2} corrected to STP is pressure difference across the membrane, s is the inside membrane area, P_1 is the atmospheric pressure, T_1 is the room temperature, V_1 is the volume flow rate of gas through the membrane during measurement at room temperature, Q_{N_2} is the permeability coefficient of N_2 permeation through the membrane of effective thickness δ_M.

[0078] Calculation of Reynolds numbers: Reynolds number is normally defined in the following way:

$$Re = \frac{D \times V \times \rho}{\mu} \quad (3)$$

Where: Re: Reynolds number; D: characteristic dimension; V: velocity; ρ: density; μ: dynamic viscosity (absolute viscosity).

[0079] The Reynolds numbers of any liquid flowing through the shell or the tube side were defined as diameter-based Reynolds number (Re_d) In the calculation of Re_d based on Eq. (3), fiber I.D. (d_i) and linear velocity are used for tube side parallel flow, and fiber O.D. and interstitial velocity/linear velocity for shell side cross flow/parallel flow.

Interstitial velocity=brine or liquid flow rate/open area for flow through the shell side (4)

[0080] The open area for flow through the shell side has been defined at the bottom of the table of FIG. **29**.

Linear velocity=flow rate/open area for flow through the (tube side/shell side) (5)

[0081] In the literature, boundary layer heat transfer coefficients are almost always estimated from empirical correlations. For laminar flow in a circular tube (i.e., fiber lumen), the Sieder-Tate equation is popularly employed (Gryta et al., 1997; Hobler, 1986):

$$Nu_c = 1.86(d_i Re_d Pr/L)^{0.33}(\mu/\mu_w)^{0.14} \quad (6)$$

where Nusselt number, $Nu_c=h_c d_i/k$, Re_d=(linear velocity)$d_i\rho/\mu$ and the Prandt**1** number, $Pr=c_p\mu/k$. Further h_c is the tube side boundary layer heat transfer coefficient, d_i is the tube/fiber I.D., k is the liquid thermal conductivity, μ_w is the liquid viscosity evaluated at the tube-wall temperature, and L is the tube length. The viscosity correction factor $(\mu/\mu^w)^{0.14}$ normally is negligible (Lawson and Lloyd, 1996b). Equation (6) is suitable for laminar tubular flow conditions (Re_d<2100).

[0082] For the calculation of the boundary layer heat transfer coefficient of liquid flowing on the shell side of cross flow hollow fiber modules, Zukauskas equation is often used for cross flow over tube bundles in heat exchangers when $10<Re_d<5\times10^2$ (Incropera and Dewitt, 2002; Kreith and Bohn, 2001):

$$Nu_h = 1.04 Re_d^{0.4} Pr^{0.36}(Pr/Pr_w)^{0.25} F_c \quad (7)$$

where Nusselt number, $Nu_h=h_h d_o/k$. Further h_h is the shell side boundary layer heat transfer coefficient, d_o represents the tube/fiber O.D., Pr_w is the Prandt**1** number evaluated at the tube-wall temperature, F_c is the tube-row correction factor. All properties except Pr_w are evaluated at arithmetic mean of the fluid inlet and outlet temperatures. These equations are provided herein at least in part to provide a basis for using Re_d in reporting experimental data even though there are potential problems due to fibers potentially moving and/or flow irregularities from the entrance section. Further the velocity used in Re_d is the interstitial velocity which takes into account the fiber packing density.

[0083] Definitions of heat transfer coefficients: At steady state, the effective heat flux at the two liquid fiber wall interfaces (see FIGS. **8***a* and **8***b*) may be described by:

$$Q = h_h A_{rh}(T_h - T_{hm}) = h_h A_{rh}\Delta T_h = h_c A_{rc}(T_{cm} - T_c) = h_c A_{rc}\Delta T_c, \quad (8)$$

where Q is the effective heat flux through the wall, ΔT_h is the temperature difference between brine bulk temperature, T_h and the temperature of the brine-wall interface on the hot side, T_{hm}, ΔT_c is the temperature difference between the temperature of the wall-cold water/brine interface, T_{cm}, and the cold water/brine bulk temperature on the cold side, T_c. In the PP hollow fiber module, the fiber wall thickness is six (6) times smaller than the inside diameter of the fiber. This significant diameter differential results in considerable difference between the outside and inside area of the hollow fibers. Accordingly, a change of the surface area for heat transfer should be taken into account. A_r represents the area ratio for the heat transferred through the fiber wall. Since the internal diameter-based surface area is being utilized as the base point, A_{rh} for the interfacial area between the hot brine and the OD is (d_o/d_i); the corresponding A_{rc} for the cold water and the ID is (d_i/d_i)=1.

[0084] Heat is conducted through the nonporous solid polymeric wall at a rate:

$$Q = h_m A_{r\ ln}(T_{hm} - T_{cm}) = h_m A_{r\ ln}\Delta T_m \quad (9)$$

where h_m is the tube wall heat transfer coefficient, ΔT_m is the trans-wall temperature difference $(T_{fm}-T_{cm})$. The surface area ratio $(A_{r\ ln})$ is defined as $(d_{r\ ln}/d_i)$ where $d_{r\ ln}$ is the logarithmic mean diameter, $((d_o-d_i)/\ln(d_o/d_i))$.

[0085] The heat transfer mechanism in a heat exchanger can be described as heat being transferred through a series of resistances; the overall heat transfer coefficient of the heat exchange process, U, is conventionally obtained as a series of resistances defined here with respect to A_{rc}: hot brine film resistance $(1/h_h)$, effective tube wall/membrane resistance $(1/h_m)$ and cold brine/distillate film resistance $(1/h_c)$:

$$UA_{rc} = \left[\frac{1}{A_{rh}h_h} + \frac{1}{A_{r\ln}h_m} + \frac{1}{A_{rc}h_c}\right]^{-1} \quad (10)$$

Therefore, the local heat flux Q can be expressed as

$$Q = \left[\frac{1}{A_{rh}h_h} + \frac{1}{A_{r\ln}h_m} + \frac{1}{A_{rc}h_c}\right]^{-1} \Delta T = UA_{rc}\Delta T \quad (11)$$

where ΔT is the local bulk temperature difference, $T_h - T_i$; the value of A_r for U depends on the basis of calculation, it can be A_{rh} or A_{rc}, or $A_{r\ ln}$. Here A_{rc} is taken as the basis.

[0086] Normally heat transfer efficiency across a given wall with a given h_m is decided by boundary heat transfer coefficients h_h and h_c. Heat transfer efficiency can be described via the temperature polarization coefficient (TPC):

$$TPC = \frac{T_{hm} - T_{cm}}{T_h - T_c} = \frac{\Delta T_m}{\Delta T} \quad (12)$$

TPC is the fraction of external applied thermal driving force that contributes to the heat transfer.

[0087] If an overall boundary layer heat transfer coefficient h is defined via

$$\frac{1}{hA_{r\ln}} = \frac{1}{A_{rh}h_h} + \frac{1}{A_{rc}h_c} \quad (13)$$

then TPC can be defined by

$$TPC = \frac{\Delta T_m}{\Delta T} = 1 - \frac{UA_{rc}}{hA_{r\ln}} \quad (14)$$

[0088] Temperature polarization has a negative influence on the heat exchange process as a consequence of the decrease in the temperature of the hot brine on the fiber surface and its increase on the fiber surface of cold side. Ideally, TPC should be equal to one (1), but usually it is lower. In order to maximize the shell side heat transfer coefficient, crossflow modules were fabricated at NJIT for testing herein.

Experimental Results and Discussion

[0089] Initially, the results of hot brine-cold water heat transfer in solid wall PP hollow fiber-based modules according to the present disclosure is described. The heat transfer performance of asymmetric UltraPES hollow fibers having an impervious interfacially polymerized coating is considered next. The use of solid PEEK-fiber based module in heat transfer studies is also described herein, as are the performances of solid wall PP hollow fiber-based devices for steam-cold tap water system. In addition, the performances of the larger module initially obtained from Membrana will be discussed. Of note, none of the modules of different fibers (but primarily of PP) described in the tables of FIGS. **19** and **20** had any measurable N_2 or H_2O vapor permeance. Thus, these hollow fiber modules were in appropriate condition for use in the heat transfer studies described herein.

[0090] FIG. **9** illustrates the performance of the PP module HEPP**1** with regard to the variation of the overall heat transfer coefficient, U, as the hot brine (4% NaCl) inlet temperature was varied at a given interstitial velocity of hot brine on the shell side and linear velocity of the cold D.I. water on the tube side. The increase of the overall heat transfer coefficient, U, with hot brine inlet temperature is due to the decrease in viscosity of the fluids, and the corresponding increase in the Reynolds number. FIG. **10** illustrates for the same system the variation of the overall heat transfer coefficient, U, with the magnitude of the interstitial velocity of the hot brine on the shell side.

[0091] From the test results reported herein, it is clear that the magnitude of the interstitial velocity strongly influences the value of the overall heat transfer coefficient, U, until a plateau is reached around 1600-1800 W/m^2-° K. This plateau is ultimately due to the combined resistance of the wall resistance and the tube-side resistance. More likely, it is due to the resistance of the solid PP fiber wall whose wall heat transfer coefficient value is in this range, which conclusion is supported by the results shown in FIG. **11**. For the same system of FIGS. **9** and **10**, FIG. **11** shows how the overall heat transfer coefficient, U, varies with the linear velocity of the cooling water on the tube side for the highest shell-side brine interstitial velocity of FIG. **10**. These test results demonstrate that, as the tube-side velocity is increased, the overall heat transfer coefficient, U, reaches a plateau of around 1800 W/m^2-° K. Therefore, the overall heat transfer coefficient, U, appears to be limited by the wall heat transfer coefficient at high values of the shell-side and tube-side velocities.

[0092] In the tests reported thus far, the hot brine was flowing always on the shell side of the HEPP**1** module in cross flow. If the hot brine flows on the tube side, the values of the overall heat transfer coefficient, U, are smaller since cross flow is generally more efficient in heat transfer at low Reynolds numbers, especially with the lower viscosity fluid (hotter fluid). This relationship is illustrated in FIG. **12**, where the cold water is in cross flow on the shell side. However, if hot brine flows on the shell side in parallel flow at a high Reynolds number, a high value of overall heat transfer coefficient, U, can be obtained, as shown in FIG. **13**. However, the limiting value of the overall heat transfer coefficient, U, is still around 1800 W/m^2-° K.

[0093] The limiting value for the overall heat transfer coefficient, U, observed for solid PP hollow fibers at high values of the convective film coefficients is most likely due to the limiting wall resistance. As previously noted, the wall heat transfer coefficient of PP solid hollow fiber of wall thickness is around

$$h_{wall} = \frac{k_{wall}}{\delta_m} = \frac{0.17}{75\times10^{-6}}\ \frac{\mathrm{W}}{\mathrm{m}^2 - ^\circ\ \mathrm{K}} = 2125\ \frac{\mathrm{W}}{\mathrm{m}^2 - ^\circ\ \mathrm{K}},$$

where the thermal conductivity of PP was assumed to be around 0.17 W/m^2-° K. A small increase in this value could change h_{wall} and U considerably. For example, a 20% increase in k_{wall} will increase h_w to 2500 W/m^2-° K. As is apparent, this value is the maximum overall heat transfer coefficient, U, that can be achieved in a solid PP hollow fiber-based exchanger where δ_m is 75 μm.

[0094] FIG. **14** illustrates the performance of a solid hollow fiber module made out of solid hollow fibers of the polymer PEEK. The overall heat transfer coefficient values, U, obtained are somewhat smaller relative to the results reported for the HEEP**1** module for two reasons. First, the ID of the fibers in the HEPEEK**1** module are smaller, so a higher pressure drop is needed for a comparable velocity/Reynolds number. In addition, the wall thicknesses of the fibers were significantly higher at 105 μm, even though their thermal conductivity were higher than that of PP. Thus, a lower tube side Reynolds number and a higher wall thickness leads to a marginally lower overall heat transfer coefficient, U. However, PEEK fibers have much higher temperature capabilities than PP fibers.

[0095] According to the present disclosure, advantageous heat transfer performance may be achieved through the use of asymmetric microporous hollow fibers that are characterized by micropores in the skin that are closed off. According to the present disclosure, less resistance would be experienced due to the wall being substantially porous.

[0096] FIG. **15** illustrates the heat transfer performances of a module built with eight (8) porous asymmetric UltraPES hollow fibers whose ID was coated with a NYLON 6-10 film by interfacial polymerization. The test results set forth in FIG. **15** were generated with a parallel flow module. At high values of the shell-side velocity of cold D.I. water and hot brine on the tube side, the overall heat transfer coefficient value, U, was around 3100 Watts/m^2-° K. This heat transfer coefficient is significantly better than results previously reported, i.e., almost 1.7 times greater than the value achieved with solid wall PP fibers. Of note, there was a small amount of salt leakage observed in this test module. The bilayer coating system described herein above is an exemplary coating system that may be employed to further reduce the potential for leakage across the fiber wall. The larger squares in FIG. **15** correspond to initial experimental runs where there was no salt leakage.

[0097] Turning next to experimental results generated in experimental procedures with steam on one side and cold tap water flowing on the other side, FIG. **16** reflects the variation of overall heat transfer coefficient, U, relative to the linear velocity of steam flowing on the tube side with tap water flowing on the shell side in cross flow. The experimental results reflected in FIG. **16** were generated with steam condensing on the tube side of module HEPP**1**, which included solid PP hollow fibers. At higher velocities of the cold tap water flow in the shell side, a plateau value of heat transfer coefficient, U, was reached at around 1600-1700 W/m^2-° K. In FIG. **17**, test results are provided for experimental runs with the HEPP**2** module where steam was condensing on the tube side and cold tap water was in cross flow on the shell side. As the linear velocity of the steam was increased, the value of the overall heat transfer coefficient, U, climbed to as much as about 1500 W/m^2-° K. These overall heat transfer coefficient values were determined via a special definition since there are two regions on the steam side: steam and condensate. These steam transfer coefficient results—as reported herein—are a composite of the heat transfer coefficients in the two regions.

[0098] Of note, condensation of steam in the disclosed solid hollow fiber heat exchange systems generates relatively small condensation water droplets. Small water droplets are advantageous in that they do not cause flow blockage through the hollow fiber. Moreover, condensation of the relatively small water droplets is effective in supplying heat/energy for transfer through the fiber wall, e.g., to the tap water flowing on the opposite side of the hollow fibers. According to exemplary embodiments of the present disclosure, prefiltration may be undertaken to ensure that impurities do not cause undesirable blockage and/or increases in pressure drop across the disclosed hollow fiber system.

[0099] Reference is made to a publication entitled "Polymeric Hollow Fiber Heat Exchangers: An Alternative for Lower Temperature Applications," authored by Dimitrios M. Zarkadas and Kamalesh K. Sirkar, which appeared in *Ind. Eng. Chem. Res.* 2004, 43, 8093-8106, incorporated herein by reference. The foregoing publication describes advantageous heat exchange applications wherein exemplary solvent/aqueous systems are employed, e.g., ethanol/water and water/aqueous solution of ethylene glycol (33% by volume). Alternative organic solvents may be employed in the disclosed heat exchange systems, as will be readily apparent to persons skilled in the art. Selection of appropriate organic solvent/polymeric solid hollow fiber systems may be influenced, at least in part, by the stability of the polymeric fibers in the presence of the proposed organic solvent. Accordingly, heat exchange applications that include organic-aqueous or organic-organic heat transfer systems may be employed according to the present disclosure.

[0100] As noted above, relatively large (1 m^2+) heat transfer modules can be obtained from Membrana based, at least in part, on preliminary experiments indicating that these heat exchanger modules were extremely efficient heat transfer devices. However, it was determined that the experimental facility would not be able to supply adequate steam or hot water for efficient heat transfer. Therefore, somewhat smaller modules with surface areas varying between 0.15 and 0.44 m^2 were obtained. FIG. **18** describes the behavior of the overall heat transfer coefficient, U, relative to the linear velocity of hot brine flowing on the shell side in parallel flow. Based on the performance results reported herein, it has been concluded that the linear velocities used here were not large enough. Overall heat transfer coefficient values of around 750 W/m^2-° K. were observed. The heat transfer surface area packing density of these modules was high, i.e., around 3000 m^2/m^3, as compared to the values of the modules fabricated at NJIT (e.g., 300 to 1500 m^2/m^3). Therefore, the product of the heat transfer coefficient, U, times the surface area/volume in this module generates a value of 2.3×10^6 W/m^3-° K., a value which is almost an order of magnitude larger than those in a conventional metallic heat exchangers ($1.3\text{-}1.5\times10^5$ W/m^3-° K.).

[0101] The table of FIG. **21** sets forth the raw data for one set of experimental runs described herein. Specifically, the data illustrated in FIG. **11** for module HEPP**1** was obtained from the raw data that is reported in the table of FIG. **21**. By comparing the raw data in the table of FIG. **21** with the plot of FIG. **11**, it will be readily apparent how the plotted heat transfer coefficient values, U, were obtained according to the present disclosure.

[0102] The table of FIG. **22** sets forth summary performance data for solid hollow fiber heat exchanges according to the present disclosure. As is readily apparent from the data

set forth in FIG. **22**, the disclosed solid hollow fiber systems are highly effective in providing advantageous heat transfer levels.

[**0103**] A polymeric hollow fiber heat exchanger module (HEPP**4**) built by Membrana, Inc. on a much larger scale than those shown in FIGS. **4** and **20** has also been tested. The structure of this device is somewhat similar to that of FIG. **5** except that the crossflow on the shell side was generated by radial flow outward from the central feed tube which was blocked at the middle. A baffle was positioned on the shell side so that the shell-side crossflow in the first half of the module flows around the baffle and comes down across the fibers in the other half of the module; the flow stream is collected and withdrawn through the other half of the central feeder tube. The total number of polypropylene (PP) solid hollow fibers was 12,100, each solid hollow fiber having an inner diameter of 430 μm and an outer diameter of 570 μm. The effective length of each hollow fiber was 24 cm, with the total length of each fiber being 33 cm. The central feed distribution tube had an outer diameter of 3.2 cm. The total available heat transfer surface area was 4 m^2 based on a fiber inner diameter for a shell side housing inner diameter of 9.7 cm, which translates to heat transfer surface area per unit volume of 22.5 cm^{-1}.

[**0104**] With reference to FIG. **23**, the results of the foregoing exemplary heat exchange apparatus for one heat transfer run are shown. In this heat transfer operation, cold city water was used on the shell side at a flow rate of 11.3 liters/min and a temperature of about 21.3-22.3° C. The plot of FIG. **23** shows heat transfer coefficients at varying brine feed temperatures on the tube side at a brine flow rate of 20 liters/min. Because of the enormous heat transfer surface area in the small exemplary heat transfer device and the higher brine flow rate (about two times that of the city water), at higher brine temperatures it is noted that the heat transfer surface area is not properly utilized. As a result, we get the highest heat transfer coefficient of around 630 W/m^2-° K. at the lowest brine temperature of ~42° C. However, the value of the overall conductance per unit volume is quite high and advantageous:

$$630\ \frac{W}{m^2 -^\circ K.} \times 2250\ \frac{m^2}{m^3} = 1.4175 \times 10^6\ \frac{W}{m^3 -^\circ K.}.$$

[**0105**] The heat exchanger modules described herein are sufficiently new that cost information is not readily available. However, the cost of such modules is likely to be comparable to or less than those of hollow fiber membrane contactors that are currently commercially available from industry manufacturers, e.g., Membrana, Inc. Further, the overall cost necessarily depends on volume of sales, the number of modules being sold to one user, and related commercial factors. Obviously, the larger the volume, the smaller the cost, varying by as much as a factor of 2-3.

[**0106**] The results described herein are novel and exciting, indicating the possibilities of polymeric hollow fiber modules made out of asymmetric polymeric solid hollow fibers for use in heat transfer. These lightweight, highly compact heat exchangers are potential candidates for heat exchange in a wide range of applications, e.g., thermal desalination processes and blood oxygenation applications. Although the heat exchanger systems of the present disclosure have been described with reference to exemplary embodiments and experimental implementations thereof, the present disclosure is not limited to such exemplary embodiments and/or experimental implementations. Rather, the heat exchanger systems of the present disclosure are susceptible to a variety of modifications, variations and/or enhancements without departing from the spirit or scope hereof. Accordingly, it is to be understood that the present disclosure extends to and encompasses such modifications, variations and/or enhancements.

Notation

[**0107**] A_r membrane area ratio for heat transfer through a membrane surface

[**0108**] A_{rc} value of A_r for cold water-tube wall interface, d_i/d_i, which is equal to 1

[**0109**] A_{rh} value of A_r for hot brine-tube wall interface, d_o/d_i

[**0110**] $A_{r\ ln}$ value of A_r for logarithmic mean membrane area, $d_{r\ ln}/d_i$, where logarithmic mean diameter, $d_{r\ ln}=(d_o-d_i)/\ln(d_o/d_1)$

[**0111**] cm centimeter

[**0112**] c_p liquid heat capacity

[**0113**] d_i fiber inside diameter (I.D.)

[**0114**] d_o fiber outside diameter (O.D.)

[**0115**] $d_{r\ ln}$ logarithmic mean diameter, $d_{r\ ln}=(d_o-d_i)/\ln(d_o/d_i)$

[**0116**] D characteristic dimension

[**0117**] D.I. deionized water

[**0118**] F liquid stream flow rate

[**0119**] F_c tube-row correction factor

[**0120**] h overall boundary layer heat transfer coefficient

[**0121**] h_c tube side boundary layer heat transfer coefficient

[**0122**] h_h shell side boundary layer heat transfer coefficient

[**0123**] h_m tube wall heat transfer coefficient

[**0124**] I.D. internal diameter

[**0125**] k liquid thermal conductivity

[**0126**] L fiber length

[**0127**] min minute(s)

[**0128**] n number of fibers in a membrane module

[**0129**] Nu_c tube side Nusselt number

[**0130**] Nu_h shell side Nusselt number

[**0131**] O.D. outside diameter

[**0132**] P_1 atmospheric pressure

[**0133**] PEEK polyetheretherketone

[**0134**] PMP poly(4-methyl-1-pentene)

[**0135**] PP polypropylene

[0136] Pr Prandt1 number

[0137] Pr_w Prandt1 number evaluated at the tube-wall temperature

[0138] Q effective heat flux through the membrane

[0139] Q_{n_2} permeability coefficient of N_2 permeation through the membrane of effective thickness δ_M

[0140] Q_{N_2}/δ_M N_2 permeance

[0141] Re Reynolds Number

[0142] Re_d diameter-based Reynolds number

[0143] s inside membrane area ($=n\pi d_i L$)

[0144] STP T_0=273.15 K, P_0=760 Torr

[0145] T_1 room temperature

[0146] T_c cold water/brine bulk temperature on the cold side

[0147] T_{cm} temperature of the tube wall-cold water/brine interface

[0148] T_h brine bulk temperature

[0149] T_{hm} temperature of the brine-tube wall interface on the hot side

[0150] TPC temperature polarization coefficient

[0151] U overall heat transfer coefficient

[0152] UltraPES Ultra-polyethersulfone

[0153] V velocity

[0154] ρ density

[0155] μ dynamic viscosity (absolute viscosity)

[0156] μ_w liquid viscosity evaluated at the tube-wall temperature

[0157] δ_M effective thickness of membrane/tube wall

[0158] ΔP_{N_2} N_2 pressure difference across the membrane

[0159] Δt liquid inlet and outlet temperature difference

[0160] ΔT bulk temperature difference between shell side and tube side

[0161] ΔT_h temperature difference between brine bulk temperature and the temperature of brine-tube wall interface on the hot side

[0162] ΔT_m trans-membrane temperature difference

[0163] ΔT_c temperature difference between temperature of tube wall-cold water/brine interface and cold water/brine bulk temperature on the cold side

1. A heat exchange system comprising:

a heat exchange module configured and dimensioned to receive a plurality of polymeric hollow fibers; and

a plurality of polymeric hollow fibers positioned in said module, wherein said plurality of hollow fibers are asymmetric, porous hollow fiber with a dense skin formed on a surface thereof.

2. A heat exchange system according to claim 1, wherein said heat exchange module is configured for cross-flow heat exchange.

3. A heat exchange system according to claim 2, wherein the heat exchange module includes at least one baffle.

4. A heat exchange system according to claim 1, wherein said heat exchange module is configured for parallel flow heat exchange.

5. A heat exchange system according to claim 1, wherein said heat exchange module is adapted for use in at least one of the following applications: a desalination application, a solar heating application, a chemical application, a biotechnology application, a biomedical application, a blood oxygenation application, or a pharmaceutical application.

6. A heat exchange system according to claim 1, wherein a dense skin is formed on a microporous surface of each of said plurality of hollow fibers.

7. A heat exchange system according to claim 1, wherein said dense skin is effective to substantially prevent liquid transmission through the wall of the hollow fiber.

8. A heat exchange system according to claim 1, further comprising liquid molecules within the porous substructure of the polymeric hollow fibers.

9. A heat exchange system according to claim 8, wherein the liquid molecules facilitate heat transfer through the hollow fiber, but are substantially prevented from passing through the wall of the hollow fiber.

10. A heat exchange system according to claim 1, wherein the heat exchange module is configured to receive process fluids and wherein the plurality of polymeric hollow fibers are substantially inert to said processing fluids.

11. A heat exchange system according to claim 1, wherein at least one of the plurality of polymeric hollow fibers is fabricated from a polymeric material selected from the group consisting of polypropylene, polyethersulfone (PES), polyamide, polyphenylenesulfide, polyimide, polyetheretherketone (PEEK), polysulfone (PS), and poly-4-methyl-1-pentene (PMP).

12. A heat exchange system according to claim 1, wherein each of the plurality of polymeric hollow fibers has a wall that is between about 20-200 μm in thickness.

13. A heat exchange system according to claim 1, wherein the dense skin is formed by an interfacial polycondensation reaction.

14. A heat exchange system according to claim 1, wherein the dense skin is formed by the following process steps: fiber pores are wetted with an aqueous monomer solution, and an organic solution having a second monomer is passed through the lumen side of the fibers to form an interfacially polymerized polyamide film on the inner diameter of the fibers.

15. A heat exchange system according to claim 1, wherein the internal surface of the asymmetric polymeric hollow fibers is provided with a bilayer coating.

16. A heat exchange system according to claim 15, wherein the first layer of the bilayer coating is formed from a reaction product of first and second reaction products.

17. A heat exchange system according to claim 15, wherein the second layer of the bilayer coating is applied over the first layer.

18. A heat exchange system according to claim 15, wherein the second layer of the bilayer coating is a cross-linked polydimethlysiloxane (PDMS).

19. A heat exchange system according to claim 18, wherein the PDMS coating is applied by introducing a silicone solution and a curing agent to the asymmetric polymeric hollow fiber lumen.

20. A heat exchange system comprising:

a heat transfer module that includes a plurality of polymeric hollow fibers, each of said plurality of polymeric hollow fibers including a wall that defines a first heat transfer side and a second heat transfer side;

a steam source that is adapted to supply steam to said heat transfer module; and

a liquid source that is adapted to supply a liquid flow to said heat transfer module;

wherein said steam is condensed on the first heat transfer side of the polymeric hollow fibers, thereby providing heat transfer energy to the liquid source on the second heat transfer side of the polymeric hollow fibers.

21. A heat exchange system according to claim 20, wherein an overall heat transfer coefficient on the order of or greater than a liquid-liquid heat exchanger is achieved.

22. A heat exchange system according to claim 20, wherein the polymeric hollow fibers define a hydrophobic polymeric surface.

23. A heat exchange system according to claim 20, wherein the steam is condensed in a drop-wise manner.

24. A heat exchange system comprising:

a heat transfer module that includes a plurality of polymeric hollow fibers, each of said plurality of polymeric hollow fibers including a wall that defines a first heat transfer side and a second heat transfer side;

a brine source that is adapted to supply brine to said heat transfer module; and

a liquid source that is adapted to supply a liquid flow to said heat transfer module;

wherein heat transfer to the brine is effected through heat transfer within the heat transfer module in connection with desalination processing of said brine.

25. A heat exchange system according to claim 24, wherein the liquid source is selected from the group consisting of brine, water and steam.

26. A heat exchange system according to claim 24, wherein the plurality of hollow fibers are asymmetric, porous hollow fibers.

27. A heat exchange system according to claim 26, wherein the asymmetric, porous hollow fibers include a dense skin on a surface thereof.

28. A heat exchange system according to claim 24, wherein the heat exchange module is adapted for at least one of cross-flow heat exchange and parallel flow heat exchange.

29. A heat exchange system according to claim 28, wherein the heat exchange module includes at least one baffle.

30. A heat exchange system according to claim 24, further comprising liquid molecules within a porous structure of the polymeric hollow fibers.

* * * * *